A discussion on turbulent and undular bores using the models from the shallow water equations and the dispersive system.

Erik Eikeland

Master's Thesis in
Hydro Dynamics

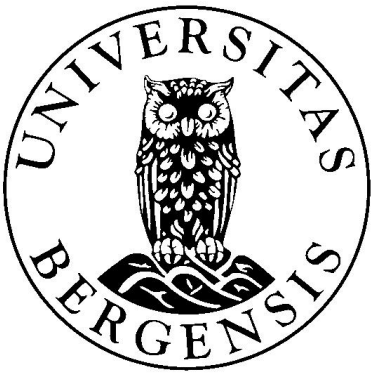

Department of Mathematics
University of Bergen
Norway

May 26, 2010

Preface

Mathematics was always my favourite subject at school, due its precise descriptions and logical nature. But it was not always clear that this would be the subject of my master thesis. In my time at the University of Bergen I have, in addition to mathematics, taken courses in physics, chemistry, statistics, informatics and even philosophy. I was about to start on a master thesis in physics when a brilliantly lectured course by Terje Espelid brought me back to mathematics, my starting point at the University.

To complete this thesis has been hard work and it would be even harder if it were not for all the help I have received. I wish to give thanks to my supervisor Henrik Kalisch, who has been a great source of both knowledge and inspiration. I also wish to thank my mother and father for their support and encouragement and my fellow students for the cheerful environment. But most of all I wish to thank my lovely Elin who has managed to get me up in the mornings and to bed at nights.

Erik Eikeland,
Bergen, May 2010

Contents

List of Figures

Chapter 1

Introduction

The bore is a wave phenomenon that occurs in channels and rivers of shallow water. Referred to as a discharge wave, a bore is generated by a sudden increase of water flow. Bores appear in certain rivers as the tide pushes water into the river mouth. The Severn river in England, the Dordogne river in France and the Qiantang river in China are all examples of rivers that display this phenomenon.

Simply described a bore is a transition between two uniform flows of different flow depth. The point of transition is referred to as the bore front. This front might be travelling or it might be stationary. However it is only in the case of a travelling front that the phenomenon is named a bore. The stationary case is named a hydraulic jump. The transition between the two states of flow is often marked by violent turbulence. But there are also bores in which no turbulence is observed. Such bores are called weak bores, as in these cases, the difference in height between the two flow depths are small. The weak bore displays a unique character not present in the turbulent bore. It carries a train of undulating waves just behind the front. For this reason it is often called the undular bore.

The bore phenomenon has been a topic of interest in hydrodynamics since the late nineteenth century. Three main experiments on discharge waves made by H. Bazin [2], H. Favre [8] and later J.A. Sandover & O.C. Zienkiewicz [18] are especially worth mentioning and we will focus on the studies of Favre. The first theories used to model the bore are those developed by Lord Rayleigh, G.G. Stokes, G.B. Ariy, G.H. Kortweg & G. de Vries, and J. Boussinesq. A good summary of these are found in G.B. Whithams book [20]. On the basis of these theories the main consensus on the bore phenomenon was drawn by T.B. Benjamin and M.J. Lighthill in the brilliant paper [3].

This thesis aims to give an introductory summary on the theory of the bore phenomenon and lay out a map for further study. In this way it ought

to serve as a good introduction for those not familiar with the subject and a good repetition for those who are.

In the following investigation two models of the bore will be presented in which water is treated as an ideal fluid. The first model is reached by assuming hydrostatic pressure. This gives the shallow water equations. These equations model the bore as a travelling discontinuity separating two uniform flow depths. The water flow is steady, conserving mass and momentum, but the water loses energy as it passes through the bore front. This energy loss was first pointed out by Rayleigh in [17] and is commonly referred to as the classical energy loss. The energy loss is a trait that coincides well with turbulent bores and the shallow water equations model these bores quite well.

The shallow water equations do not model the undular bores as they would not sustain the undulating waves behind the bore front. A second model is based on a dispersive system. This is an extension of the shallow water equations where, effectively, the treatment of pressure is refined. It leads to various Boussinesq systems and in a specialized case, of all fluid moving in one direction, it leads to the well know KdV equation. Modelling a bore-like initial value by a dispersive system brings out the undulations behind the bore front, however it does not capture the full nature of the undular bore itself.

The nature of the undular bores is found through experiments. Of the three experiments mentioned above, we focus on the work of Favre published in his book [8]. From this study Favre concluded, as pointed out by Keulegan and Patterson in [11], that:

1. *The undulations are not formed immediately, but require a certain amount of time to establish themselves.*

2. *After the undulations are formed, they are of similar size and shape.*

3. *The final configuration is a stable one*[1]*.*

4. *The height of the undulation at x is independent of θ, the time in which the flow is established, for a considerable range of values of x, provided $\theta U/x < 0.2$, U being the travelling speed of the front. In other words within certain limits, a discharge which is not created instantaneously will behave like a theoretically sudden increase of flow.*

5. *The wave length of the undulations depends only on the mean height of the layer above the primitive surface. The former decreases as the latter increases.*

[1] By this they mean that the flow has become steady.

The dispersive model agrees with these observations in all but case 3 and 5. It does not show a rapidly stabilizing effect, i.e. the bores of the dispersive model does not obtain the steady flow found in experimental bores. And the model wave length seems independent of the mean height of the layer above the primitive surface.

In [3] Benjamin and Lighthill develop the dispersive model in a new way that illuminates the roll of mass flow, momentum flow and energy. Relaying on the experimental results, they assume a steady flow at the bore front and seek solutions of travelling waves. This assumption, might be unfortunate, as the dispersive model has trouble attain steady flow when simulating a bore like initial value. They find the undulations behind the front to be one of three types of waves; sinusoidal, cnoidal or solitary. However only solitary waves are allowed if conservation of energy is to be assumed. The experimental observations suggest that the undulations are cnoidal. On this basis Benjamin and Lighthill conclude that the undular bore must suffer an energy loss through the bore front similar to the classical loss. Sturtevant [19] continues this line of reasoning and tries to calculate the loss. His calculations reveal the surprising result that the flow does not suffer an energy loss but an energy gain. This result however is explainable if frictional effects of the bottom are taken into account.

In this thesis we support the conclusion that adding frictional effects of the boundary will improve the dispersive model of the undular bore. But the arguments leading to this conclusion will be debated. The fact that the undular bore quickly establishes steady flow while the dispersive model does not, shows that model needs further work. But it also illustrates the problem of Benjamin & Lighthill and Sturtevants reasoning. Assuming steady flow and applying this to a model that, for the given phenomenon, does not attain it, is likely to give an invalid argument. The model needs to be modified in such a way that a simulated bore quickly obtains steady flow. Only then an argument similar to Benjamin and Lighthills can be applied.

Finally we wish to clarify the idea of the classical energy loss. This energy loss seems to be a source of confusion. The consensus is that the fluid needs to loose energy as it passes through the bores transition between the two flow depths, the bore front, however this idea is most likely a phantom of the shallow water equations. A closer reading of Rayleighs paper [17], where the energy loss was introduced, indicates that the use of the dispersive model removes the need for an energy loss. The dispersive system, which incorporates the fluids oscillation in the z-direction, appears to give the fluid a dynamical property such that it contain its energy as it passes through the bore front. Further evidence of this is given in [1] where Alfatih and Kalisch, using a dispersive system, preforms a numerical study of bore-like

Figure 1.1: The two bores are from the Severn and the Qiantang river. The first picture is from the Severn river, showing an undular bore with marked oscillations behind the bore front. The picture is found at the serven bore page www.serven-bore.co.uk. The second picture is a vastly turbulent bore in the Qiantang river. Notice the difference in flow depths and the turbulent front dividing them.

initial values. Their study show that the simulated fluid conserve energy. With this result we may conclude that our focus should not be on the bores energy loss as such but rather on it ability to attain steady flow.

Preliminary equations for water waves.

In the following explanations we will use a Cartesian coordinate system with the coordinates (x, y, z). The x and y axes will be the horizontal axes and the z axis will be the vertical axis. The vector $\mathbf{u} = (u, v, w)$ will represent the flow of the fluid in the spatial directions where u is the flow in the x direction, v the flow in the y direction and so on. The fluid we consider is water. This is commonly seen as an ideal fluid. By this we mean that it is incompressible, homogeneous, non-viscous and irrotational. These ideal properties of water will greatly simplify future equations.

As water is homogeneous and incompressible, the density of water ρ is constant. The principle that water does not compress nor vanish but only moves is expressed by the continuity equation. The continuity equation at a point becomes $u_x + v_y + w_z = 0$. Which in short is:

$$\nabla \cdot \mathbf{u} = 0 \tag{1.1}$$

The motion of water is described by an equation of motion. Any equation of motion is based on Newtons second law of physics

$$ma = F_{res} \tag{1.2}$$

where m is matter, a is acceleration and F_{res} is the sum of all forces. Matter changes its motion according to the sum of forces acting upon it. In this study gravity and pressure are the forces acting upon water. Pressure is a force acting on the water surface[2]. It can be divided into a force normal to the surface and a force tangential to the surface. Since we state that water is non-viscous the tangential force on water must be zero. The normal force can be expressed as the gradient of pressure $F_p = -\nabla p$. Gravity is a force acting on the entire fluid. Such a force is called a body force. Gravity is a conservative body force and can thus be expressed as the gradient of a potential $F_g = -\rho\nabla\Pi$ where $\Pi = gz$ and g is the intensity of gravity.

Summed up, the equation of motion used for water as an ideal fluid is the Euler equation

$$\rho\frac{D\mathbf{u}}{Dt} = -\nabla p - \rho\nabla\Pi \tag{1.3}$$

where we will call $\frac{D}{Dt} = \frac{\partial}{\partial t} + \mathbf{u}\cdot\nabla$ a material derivative. By a material derivative we indicate that we are following a fluid particle and that we are interested in the change that this particle is experiencing. The Euler equation is a vector equation which written in full becomes:

$$\rho(u_t + uu_x + vu_y + wu_z) = -p_x \tag{1.4}$$

$$\rho(v_t + uv_x + vv_y + wv_z) = -p_y \tag{1.5}$$

$$\rho(w_t + uw_x + vw_y + ww_z) = -p_z - \rho g \tag{1.6}$$

It contains 4 unknowns (u, v, w) and p and together with the continuity equation it expresses 4 different equation that constitute a complete set of equations.

Assume that water is flowing in a flat bottomed lake of infinite length and width. Let H_0 be the undisturbed water depth and $\eta(x, y, t)$ be the surface deviation from the undisturbed depth. Now define $h(x, y, t) = \eta(x, y, t) + H_0$ as the total water depth. Two Boundary types are then treated. The free surface boundary between water and air and the solid fixed boundary between water and the bottom. For the free surface two principles apply. The kinematic condition

$$\eta_t + u\eta_x + v\eta_y = w \tag{1.7}$$

that water does not leave the free surface and the dynamic condition

$$p = p_0 \quad \text{at } z = h(x, y, t) \tag{1.8}$$

[2]This is a general statement of the pressure force. Therefore in this case surface is to be interpreted in the broadest possible sense, including the surfaces of arbitrary cross-sections.

that the pressure at the surface is equal to the atmospheric pressure p_0. In addition no water pass through a solid fixed boundary. For a flat horizontal bottom this gives

$$w = 0, \quad \text{at } z = 0. \tag{1.9}$$

This concludes the basics for water wave equations. Fluid mechanical terms, not mentioned here, will appear with brief explanations during this thesis. More thorough explanations are found in books of fluid mechanics such as [13].

Chapter 2

The shallow water equations

In the study of bores and hydraulic jumps we assume that water is flowing in an infinite and narrow channel with a flat horizontal bottom. We place the coordinate system with the x-axis at the bottom in the direction of flow and the z-axis in the vertical direction. We assume that there is no flow in the y-direction as the channel is narrow. This gives us a two dimensional system in x and z. The assumption characterizing the shallow water equations is that the waves are long compared to the water depth. From this we may neglect the flow in the z direction and the horizontal velocity is uniform at each cross-section of the channel. Applying these simplifications to the Euler equations we retain (1.4) and (1.6) and they become

$$\rho(u_t + uu_x) = -p_x \tag{2.1}$$

$$0 = -p_z - \rho g. \tag{2.2}$$

Let H_0 be the undisturbed water depth and $\eta(x,t)$ be the surface deviation from the undisturbed depth. Now define $h(x,t) = \eta(x,t) + H_0$ as the total water depth. If h is integrated between to vertical cross-sections of the channel, the integrand is the volume of water between the cross-sections per unit width. Multiplying this with ρ we get the mass of water per unit width. Since h is the only variable in this calculation, and the cross-sections were chosen arbitrarily, h will often be referred to as the mass of the fluid.

The equation of continuity in the introduction gives continuity at a point. Continuity at a vertical cross-section of the channel is an integrated form of (1.1)

$$\begin{aligned} &\textstyle\int_0^h \left\{\frac{\partial u}{\partial x} + \frac{\partial w}{\partial z}\right\} dz = 0 \\ &= \textstyle\frac{\partial}{\partial x}\int_0^h u dz + [w]_0^h - [u]_{z=h}\frac{\partial h}{\partial x}, \end{aligned} \tag{2.3}$$

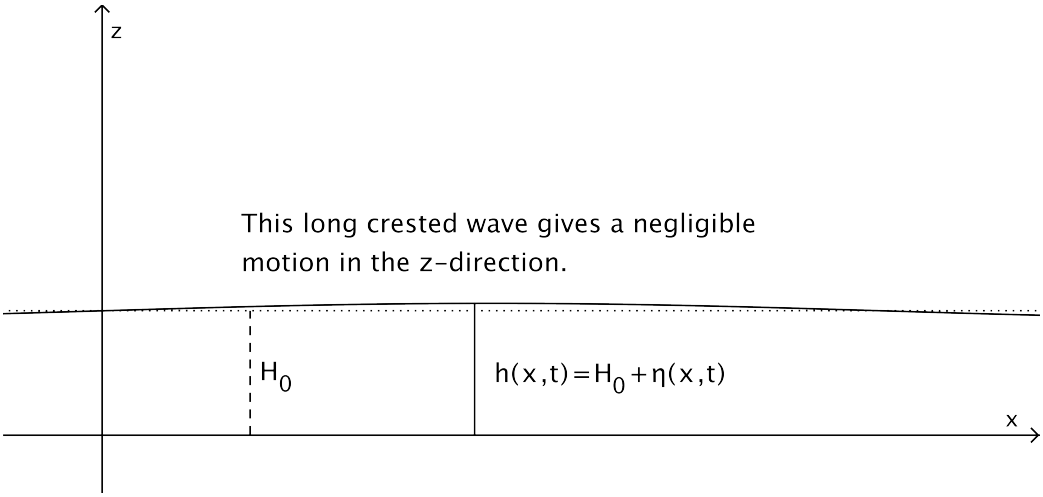

Figure 2.1: An illustrating profile of water in a channel. The stapled line is the undisturbed depth, i.e. where the water would be if it suffered no disturbance. The full line indicate the water surface. The long wave shown gives a negligible motion in the z-direction.

which using the boundary conditions (1.8) and (1.9) gives

$$\frac{\partial}{\partial x}\int_0^h u dz + \frac{\partial h}{\partial t} = 0. \tag{2.4}$$

Since u is independent of z the continuity equation becomes

$$h_t + (hu)_x = 0 \tag{2.5}$$

expressing the conservation of mass. That (2.5) expresses the same principles as (1.1) is checked by integrating (2.5) between two fixed cross-sections. The resulting expression

$$\frac{d}{dt}\int_{x_1}^{x_2} h dx = (hu)|_{x_2}^{x_1} \tag{2.6}$$

states that the change of mass with time, between the two cross-sections, is given by the net mass flux. The water does not compress nor vanish, it moves.

From (2.2) we see that the pressure is hydrostatic

$$p - p_0 = \rho g(h - z). \tag{2.7}$$

By hydrostatic pressure we mean that the water pressure is given by gravity alone, which naturally follows as flow in the vertical direction is neglected.

Using this hydrostatic pressure in (2.1) with ρ as unity gives us

$$u_t + uu_x + gh_x = 0 \tag{2.8}$$

the conservation of momentum. Together (2.5) and (2.8) constitute the shallow water system.

$$\begin{aligned} h_t + (hu)_x &= 0 \\ u_t + uu_x + gh_x &= 0 \end{aligned} \tag{2.9}$$

2.1 Steady flow of the shallow water system

The following section is inspired by Rayleighs paper [17]. Assume that the channel flow is steady. This means that in an inertial frame of reference surface waves are given as travelling waves, e.g. waves travelling without change of form. By placing the reference frame in wave fixed coordinates the shallow water equations (2.9) become time independent.

$$\begin{aligned} (hu)_x &= 0 \\ uu_x + gh_x &= 0 \end{aligned} \tag{2.10}$$

Take two vertical cross-sections of the channel at x_1 and x_2. Let u_1 and u_2 be the two corresponding flow velocities, and let h_1 and h_2 be the two corresponding flow depths. Let $h_1 = H_0$ and $h_2 = H_0 + \eta_0$ where h_0 is the undisturbed water depth and η_0 is an elevation of the fluid above the undisturbed water depth. By the equation of continuity in (2.10) we have

$$u_2(H_0 + \eta_0) - u_1 H_0 = 0 \tag{2.11}$$

The equation of motion in (2.10) gives

$$\frac{1}{2}(u_1^2 - u_2^2) - g\eta_0 = 0 \tag{2.12}$$

Using (2.11) to express u_2 in terms of u_1 we get $u_2 = \frac{u_1 H_0}{H_0 + \eta_0}$. Substituting u_2 in (2.12) by this expression gives

$$(\frac{u_1^2}{H_0} \cdot \frac{1 + \eta_0/2H_0}{(1 + \eta_0/H_0)^2} - g)\eta_0 = 0 \tag{2.13}$$

From this Rayleigh draws the following conclusions: "*If, now, the ratio* η_0/H_0 *be very small, the coefficients of* η_0 *becomes*

$$\frac{u_1^2}{H_0} - g, \tag{2.14}$$

Figure 2.2: Three pictures of a hydraulic jump created by here at University of Bergen by letting water run from the tap down on a flat surface. As the water hits the flat surface it carries a lot of momentum. Shooting out to the sides it obtains a supercritical flow and shortly after preforms a hydraulic jump. The jump is marked by a region of turbulence and beyond this region the surface is calm.

and we conclude that the condition of a free surface is satisfied, provided $u_1^2 = gH_0$. *This determines the rate of flow, in order that a stationary wave may be possible, and gives, of course, at the same time the velocity of a wave in still water.*

Unless η_0^2 *may be neglected, it is impossible to satisfy the conditions of a free surface for a stationary long wave, which is the same as saying that it is impossible for a long wave of finite height to be propagated in still water without change of type.*

A flow in which $u > \sqrt{(gH_0)}$ is called supercritical. As it does not satisfy the free surface condition it is unstable and the water level will rise. This increase in water depth is rapid and is called a hydraulic jump. The hydraulic jump lowers the flow speed and increases the the limit for supercritical flow. The phenomenon is often observed below weirs and dams. Something of the kind may also be seen whenever a stream of water from a tap strikes a horizontal surface.

2.1.1 The classical hydraulic jump

In the theory of hydraulic jumps, water is flowing super critically before undergoing a relatively rapid increase of water depth from H_0 to $H_0 + \eta_0$, η_0 being the size of the jump. The depth increase is stationary and often associated with a very turbulent mixing of water, producing a significant energy loss. The increase of the water depth is so rapid that it is modelled as a discontinuity.

Lets assume that a channel is below a dam. Let the dam be an infinite reservoir of water. Let water run from the dam into the channel at a supercritical flow u_l. At x_0 it undergoes a jump from H_0 to $H_0 + \eta_0$ changing

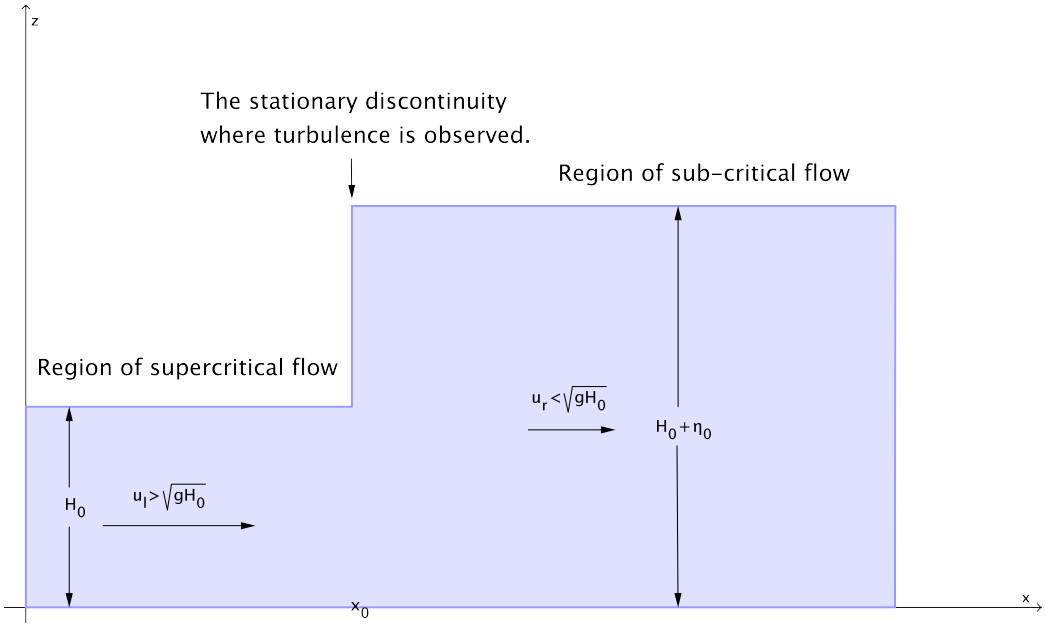

Figure 2.3: Hydraulic jump. The hydraulic jump consists of three parts: A region of supercritical flow, a jump discontinuity and a region of sub-critical flow.

flow velocity from u_l to u_r. The subscripts l and r indicates that the values are to the left and to the right of the jump. All water arriving at x_0 has experienced the same amount of work, down to a slight difference in pressure due to minor surface wave variations. These variations are neglected as there are no surface waves to speak of in a supercritical flow. From this physical argument we assume that the flow is steady as it passes through x_0. A steady flow conserves mass and momentum[1]. Conservation of mass given by (2.11)

$$u_l H_0 = u_r(H_0 + \eta_0) = Q$$

states that the mass flux is the same in any vertical cross-section. Conservation of momentum states

$$Q(u_l - u_r) = \frac{1}{2}g((H_0 + \eta_0)^2 - (H_0)^2) \tag{2.15}$$

that the difference in momentum flux at the jump is due to the difference in pressure left and right of the jump. By these equations u_l and u_r are determined and we have:

$$u_l^2 = \frac{1}{2}g(2H_0 + \eta_0)(\frac{H_0 + \eta_0}{H_0}), \qquad u_r^2 = \frac{1}{2}g(2H_0 + \eta_0)(\frac{H_0}{H_0 + \eta_0}). \tag{2.16}$$

[1]The conservation of momentum needs the flow to be frictionless. In a non-viscous fluid frictionless flow is guaranteed.

Considering the energy we see that the difference of work done on a fluid particle at the two ends is $(\frac{1}{2}g\eta_0)$. The volume flow passing through the jump per unit time per unit width is Q. The product $Q(\frac{1}{2}g\eta_0)$ is the difference of work done on the fluid passing trough the jump per unit time and width. The difference in kinetic energy per unit time and width is $Q(\frac{1}{2}u_l^2 - \frac{1}{2}u_r^2)$ and finally the difference in potential energies per unit time and width is $Q(\frac{1}{2}g\eta_0)$. The total loss of energy is then

$$\begin{aligned} Q(g\eta_0 + \frac{1}{2}u_l^2 - \frac{1}{2}u_r^2) &= Q(g\eta_0 + \frac{1}{4}g(2H_0 + \eta_0)(\frac{H_0 + \eta_0}{H_0} - \frac{H_0}{H_0 + \eta_0}) \\ &= Q\frac{g\eta_0^3}{4H_0(H_0 + \eta_0)}. \end{aligned} \tag{2.17}$$

per unit time and width which is the classical energy loss, first shown by Rayleigh.

If an observer was standing by the channel at x_0 he would see that the water coming from the dam was rising from a depth H_0 to a depth $H_0 + \eta_0$ creating a lot turbulence at x_0 as the water was ridding it self of excess energy.

2.2 The advection equations and conservation laws

Before we analyse the shallow water equations any further we will look at some general properties of advection equations[2]. Let u be a property of the fluid like the mass or the flow velocity. If we integrate the fluid property between two cross sections of the channel and take the derivative of this integral with respect to time we have an expression of the fluid property‘s change with time inside a fixed volume. If the property studied is conserved then the change must be given by the flux of this property through the boundary of the volume. Let x_1 and x_2 be two cross-sections in the channel and the flux of u be expressed as $f(u)$. Then we have

$$\frac{d}{dt}\int_{x_1}^{x_2} u(x,t)dx = f(u(x_1,t)) - f(u(x_2,t)). \tag{2.18}$$

By moving the flux terms to the left hand side and expressing them as an integral of x we get a nicer expression. With fixed limits we can move the

[2]The theory on advection equations, presented here, is tailored for our discussion. For further reading we suggest [15]

derivative of time inside the integral to the left

$$\int_{x_1}^{x_2} u_t + (f(u))_x dx = 0. \tag{2.19}$$

The size of the fixed volume is arbitrarily chosen. If we assume that both u and $f(u)$ are smooth we may take the limit of the integral above as its volume goes to zero. We then get the equation in differential form

$$u_t + (f(u))_x = 0. \tag{2.20}$$

We call this an advection equation. It states that the change of the fluid property in a point is given by the net flow of the property at that point. Later we will show that under certain assumptions we may treat the shallow water equations as a system of equations on this form.

The solution of an advection equation is found through the study of its characteristics. In the one dimensional case the material derivative is given as

$$\frac{D}{Dt}u = u_t + x'(t)u_x \tag{2.21}$$

where $x'(t)$ is the travelling speed of the property. Writing (2.20) on this form

$$u_t + f'(u)u_x = 0, \tag{2.22}$$

it follows that if $f'(u)$ plays the same role as $x'(t)$ then $\frac{D}{Dt}u = u_t + f'(u)u_x = 0$ and the solution of $u(x,t)$ is constant along each ray $x - f'(u)t = x_0$ called the characteristics of the equation.

The solutions of the advection equations are thus largely determined by the flux of the fluid property's dependence on the fluid property. Let us consider the initial value problem:

$$\begin{aligned} u_t + (f(u))_x &= 0 \\ u(x,0) &= u_0(x) \end{aligned} \tag{2.23}$$

with the simple flux relation $f(u) = au$ where a is a constant. We get the characteristics $x - at = x_0$. The initial value $u_0(x)$ can be viewed as a distribution of a fluid property in space. Given any particular value of x we get the particular property at that point. Now following a characteristic the fluid property is unaltered. All the characteristics are straight lines with the same slope a. This leads us to conclude that the initial distribution is unaltered, thus $u(x,t) = u_0(x - at)$ is a solution to the problem. However $f(u)$ need not have such a simple form.

What happens in a non-linear case? Let $f(u) = \frac{1}{2}u^2$. The characteristics become $x - u_0(x_0)t = x_0$. Again the characteristics are straight lines but what about the slope of these lines? The slope varies with the initial distribution of the fluid property. If $u_0'(x) < 0$ for any x then there exists a point where the characteristics will cross. This means that the solution $u(x,t)$ becomes multivalued and we have a shock condition.

2.3 The shallow water system as advective equations.

We suggested that the shallow water system (2.9) is a system of advective equations. This is shown by assuming a relation between h and u giving $h = h(u)$ and $u = u(h)$. Such a relation is already indicated in the above section of hydraulic jumps. This way the shallow water system becomes

$$\begin{aligned} h_t + (u'(h) + u)h_x &= 0 \\ u_t + (u + gh'(u))u_x &= 0 \end{aligned} \tag{2.24}$$

Further we claim that the conservation expressed by the two equations applies to the same particles. From this claim it follows that the characteristics of the two equations are equal. They are equal if and only if

$$(u'(h) + u) = (u + gh'(u)) \tag{2.25}$$

hold. Let $u = 2\sqrt{gh} + C$ where C is a constant be the relation between u and h. Then $u' = \frac{g}{\sqrt{gh}}$, $h = \frac{u^2 - 2uC + C^2}{4g}$ and $h' = \frac{u}{2g} - \frac{C}{2g}$. Using these relations in the above we get

$$u + \frac{hg}{\sqrt{gh}} = u + \frac{u}{2} - \frac{C}{2}. \tag{2.26}$$

Inserting for u we get

$$3\sqrt{gh} + C = 3\sqrt{gh} + C \tag{2.27}$$

which is the slope of the characteristics for the system. We determine C by claiming that $u = 0$ as $\eta = 0$ this gives $C = -2\sqrt{gH_0}$. From this we see that the solution of a simple wave moving to the right is given as:

$$\begin{aligned} h &= h(\xi) \\ u &= 2\sqrt{gh(\xi)} - 2\sqrt{gH_0} \\ x &= \xi + \left\{3\sqrt{gh(\xi)} - 2\sqrt{gH_0}\right\} t \end{aligned} \tag{2.28}$$

As long as $h'(\xi) < 0$ there will be crossing characteristics. Thus all shallow water waves carrying an increase in elevation will break.

2.4 Shock solutions

Any solution of a simple wave in the shallow water system develops a discontinuity and becomes multivalued. We say that the wave is breaking at the discontinuity. Physically we are content as long as the conservation laws are fulfilled. Mathematically a multivalued solution is unacceptable but a discontinuity is manageable. A discontinuity is present on an infinitely small domain. If the conservation laws are expressed on integral form, that is over a volume containing the discontinuity, the presence of the discontinuity, living on an infinitely small domain, is not significantly important. The main task is to make sure that the integral expressions satisfy the conservation laws. This is done by continually moving the discontinuity and we call the speed at which the discontinuity moves for the shock speed. The solution of an advection equation expressed in this manner is called a weak solution.

2.4.1 Weak solutions

Recall that (2.20) is on differential form. It requires that u is smooth. Now define a set of test functions $\phi = \phi(x,t)$ where $\phi \in C_0^1(\mathbb{R}\times\mathbb{R})$. Here C_0^1 is the space of function that are continuously differentiable with compact support. Multiplying ϕ into (2.20) and integrating over the entire domain we get

$$\int_0^\infty \int_{-\infty}^\infty \phi u_t + \phi(f(u))_x dxdt = 0 \tag{2.29}$$

and integrating this expression by parts yield

$$\int_0^\infty \int_{-\infty}^\infty \phi_t u + \phi_x(f(u))dxdt = -\int_{-\infty}^\infty \phi(x,0)u(x,0)dx. \tag{2.30}$$

Having transferred the derivatives to the test function in (2.30) u no longer needs to be smooth. The function $u(x,t)$ is called a weak solution of the advection equation if (2.30) is satisfied for all functions $\phi \in C_0^1(\mathbb{R}\times\mathbb{R}^+)$.

2.4.2 The Riemann Problem

A discontinuity in its simplest form is given in the Riemann problem. Let the initial values for mass and momentum in an infinite channel be

$$h_0 = \begin{cases} h_l & x<0 \\ h_r & x>0 \end{cases} \quad (uh)_0 = \begin{cases} (uh)_l & x<0 \\ (uh)_r & x>0 \end{cases} \tag{2.31}$$

where $h_l > h_r$ and $(uh)_l > (uh)_r$ and the subscripts l and r indicates that the values are to the left and to the right of the discontinuity. Let U denote

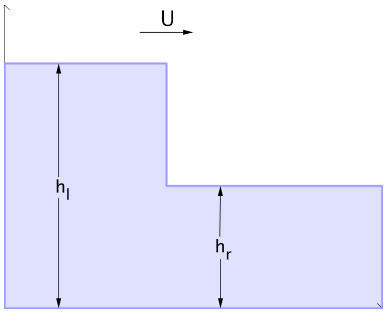

Figure 2.4: The weak solution to the Riemann problem travelling to the right with shock speed U.

the shock speed. For mass the shock speed is given as $U = \frac{(uh)_l - (uh)_r}{h_l - h_r}$ and for momentum it is $U = \frac{(u^2h + \frac{1}{2}gh^2)_l - (u^2h + \frac{1}{2}gh^2)_r}{(uh)_l - (uh)_r}$. That these shock speeds are equal follow from our assumption that the two conservation equations have equal characteristics. The weak solution has the form of a discontinuity travelling at shock speed:

$$h = \begin{cases} h_l & x < Ut \\ h_r & x > Ut \end{cases} \quad uh = \begin{cases} (uh)_l & x < Ut \\ (uh)_r & x > Ut \end{cases} \tag{2.32}$$

Using (2.30) we can test if this is a weak solution. The following calculation shows that (2.30) is the weak solution conserving matter.

$$\begin{aligned}
&\int_0^\infty \int_{-\infty}^\infty \phi_t h + \phi_x (uh) dx dt \\
&= \int_0^\infty \int_{-\infty}^{Ut} \phi_x (uh)_l dx dt + \int_0^\infty \int_{Ut}^\infty \phi_x (uh)_r dx dt \\
&+ \int_{-\infty}^0 \int_0^\infty \phi_t h_l dt dx + \int_0^\infty \int_{\frac{x}{U}}^\infty \phi_t h_l dt dx + \int_0^\infty \int_0^{\frac{x}{U}} \phi_t h_r dt dx \\
&= \int_0^\infty \{(uh)_l - (uh)_r\} \phi(Ut, t) dt + \int_0^\infty \{h_r - h_l\} \phi(x, \frac{x}{U}) dx \\
&- \int_{-\infty}^0 \phi(x, 0) h_l dx - \int_0^\infty \phi(x, 0) h_r dx \\
&= - \int_{-\infty}^0 \phi(x, 0) h_l dx - \int_0^\infty \phi(x, 0) h_r dx
\end{aligned}$$

The last expression is reached by a variable change of the second integral in the second to last equation. The weak solution exists only for the shock speed stated above. Confirming the weak solution for momentum is similar.

Generally the Rankine-Hugoniot jump condition gives the shock speed:

$$U = \frac{f(u_l) - f(u_r)}{u_l - u_r} = \frac{[f]}{[u]} \tag{2.33}$$

Here u is a fluid property and f the flux. Worth noting is that the equation above may be written as

$$U[u] = [f]$$

stating that the change of fluid property inside a control volume is equal to the net flux of that property. Based on the Rankine-Hugoniot jump condition we can restate the shallow water equations in which a discontinuity is fitted in:

$$-U[h] + [uh] = 0 \tag{2.34}$$

$$-U[uh] + [u^2h + \frac{1}{2}gh^2] = 0 \tag{2.35}$$

An observant reader might suggest that (2.35) is not the equivalent of (2.8). If uh is smooth (2.35) can be given in differential form:

$$(uh)_t + (u^2h + \frac{1}{2}gh^2)_x = 0 \tag{2.36}$$

It is easy to check that (2.8) follow from (2.36) as long as (2.5) holds, however this requires uh to be smooth.

2.5 The travelling bore and the hydraulic jump

The weak solution (2.32) is the shallow water equations model for the bore. The bore is then a travelling discontinuity, with shock speed U. In a reference frame moving at the shock speed U the bore and the hydraulic jump appears to be the same. This is confirmed by calculating the energy loss for the bore.

2.5.1 Energy of the bore

Every particle has mechanical energy. The kinetic energy is $\frac{1}{2}u^2$ and the potential is gh, with $\rho = 1$. The total energy of a cross-section is

$$\int_0^h \frac{1}{2}u^2 + (gh)dy = \frac{1}{2}u^2h + \frac{1}{2}gh^2 \tag{2.37}$$

Integrating this from x_1 to x_2 we get the energy inside a volume. If the energy is conserved, the change of energy with time inside the volume is given by the net flux.

$$\frac{d}{dt}\int_{x_1}^{x_2} \frac{1}{2}u^2h + \frac{1}{2}gh^2 dx = (\frac{1}{2}u^3h + ugh^2)|_{x_2}^{x_1} \tag{2.38}$$

Rewriting this equation we get

$$\int_{x_1}^{x_2} (\frac{1}{2}u^2h + \frac{1}{2}gh^2)_t + (\frac{1}{2}u^3h + ugh^2)_x dx = 0. \tag{2.39}$$

Applying the argument that the volume is chosen arbitrarily we deduce that the conservation of energy is given by

$$(\frac{1}{2}u^2h + \frac{1}{2}gh^2)_t + (\frac{1}{2}u^3h + ugh^2)_x = 0. \tag{2.40}$$

Since the shallow water equations model the bore as a travelling discontinuity the energy conservation must be expressed as a shock equation

$$[\frac{1}{2}u^3h + ugh^2] - U[\frac{1}{2}u^2h + \frac{1}{2}gh^2] = 0. \tag{2.41}$$

This equation is stating that the difference between net flux and the change of energy inside the control volume is zero. However we suspect the bore to lose an amount of energy similar to the classical loss of the hydraulic jump. To calculate the left hand side of (2.41) we need to rewrite (2.34) and (2.35) with respect to U and u_l. From (2.34) it follows that

$$u_l = u_r\frac{h_r}{h_l} + U\frac{(h_l - hr)}{h_l} \tag{2.42}$$

We use this in (2.35) to get an quadratic expression for the shock speed.

$$\begin{gathered} U^2 - 2u_rU + u_r^2 - \tfrac{g}{2h_r}h_l(h_l + h_r) = 0 \\ U = u_r \pm \sqrt{\tfrac{gh_l(h_l+h_r)}{2h_r}} \end{gathered} \tag{2.43}$$

For $u_r = 0$ we choose U to be positive. Inserting this in (2.42) we get the mass and momentum conservation expressed in terms of the shock speed and the fluid flow on the left hand side:

$$U = u_r + \sqrt{\tfrac{gh_l(h_l+h_r)}{2h_r}}, \quad u_l = u_r + (\tfrac{h_l-h_r}{h_l})\sqrt{\tfrac{gh_l(h_l+h_r)}{2h_r}} \tag{2.44}$$

We are now ready to check if (2.41) is correct. As convenient abbreviations we will use $\alpha = \sqrt{\frac{gh_l(h_l+h_r)}{2h_r}}$ and $\beta = (\frac{h_l-h_r}{h_l})$.

$$
\begin{aligned}
U &= u_r + \alpha & \tfrac{1}{2}g(h_l^2 - h_r^2) &= \beta\alpha^2 h_r \\
u_l &= u_r + \beta\alpha & Uu_r^2 &= u_r^3 + u_r^2\alpha \\
u_l^2 &= u_r^2 + 2u_r\beta\alpha + \beta^2\alpha^2 & Uu_l^2 &= u_r^3 + 2u_r^2\beta\alpha + u_r\beta^2\alpha^2 \\
u_l^3 &= u_r^3 + 3u_r^2\beta\alpha + 3u_r\beta^2\alpha^2 + \beta^3\alpha^3 & &+u_r^2\alpha + 2u_r\beta\alpha^2 + \beta^2\alpha^3
\end{aligned}
$$

$$
\begin{aligned}
&[\frac{1}{2}u^3h + ugh^2] - U[\frac{1}{2}u^2h + \frac{1}{2}gh^2] \\
&= \frac{1}{2}(u_l^3h_l - u_r^3h_r) + g(u_lh_l^2 - u_rh_r^2) - \frac{1}{2}U(u_l^2h_l + u_r^2h_r) - U\beta\alpha^2h_r \\
&= \frac{1}{2}(h_l - h_r)u_r^3 + \frac{1}{2}h_l(3u_r^2\beta\alpha + 3u_r\beta^2\alpha^2 + \beta^3\alpha^3) + 2\beta\alpha^2u_rh_r + \beta\alpha gh_l^2 \\
&- \frac{1}{2}h_l(u_r^3 + 2u_r^2\beta\alpha + u_r\beta^2\alpha^2 + u_r^2\alpha + 2u_r\beta\alpha^2 + \beta^2\alpha^3) \\
&+ \frac{1}{2}h_r(u_r^3 + u_r^2\alpha) - \beta\alpha^2u_rh_r - \beta\alpha^3h_r \\
&= \frac{1}{2}u_r^2\beta\alpha h_l + u_r\beta^2\alpha^2h_l + \frac{1}{2}\beta^2\alpha^3(\beta - 1)h_l \\
&+ \beta\alpha^2u_r(h_r - h_l) + \beta\alpha gh_l^2 + \frac{1}{2}\alpha u_r^2(h_r - h_l) - \beta\alpha^3h_r \\
&= \frac{1}{2}\beta^2\alpha^3(\beta - 1)h_r + \beta\alpha gh_l^2 - \beta\alpha^3h_r \\
&= \beta\alpha gh_l^2 - \frac{1}{4}\beta^2\alpha gh_l(h_l + h_r) - \frac{1}{2}\beta\alpha gh_l(h_l + h_r) \\
&= \frac{1}{2}\beta\alpha gh_l(h_l - h_r) - \frac{1}{4}\beta^2\alpha gh_l(h_l + h_r) \\
&= \frac{1}{2}\alpha g(h_l - h_r)^2(1 - \frac{h_l + h_r}{2h_l}) = \frac{\alpha g}{4h_l}(h_l - h_r)^3
\end{aligned}
$$

We have found that (2.41) is not correct and we rewrite it as

$$[\frac{1}{2}u^3h + ugh^2] - U[\frac{1}{2}u^2h + \frac{1}{2}gh^2] = \frac{\alpha g}{4h_l}(h_l - h_r)^3 \tag{2.45}$$

Say that we have a control volume containing the discontinuity of the bore. The equation above states that the net energy flux, subtracted the change of energy inside the volume due to shock speed, leaves a surplus of energy as long as $h_l > h_r$. The relation $h_l > h_r$ coincides with our choice of $U > 0$.

This means that the control volume accumulates energy. In other words there needs to be a loss of energy inside the control volume. The size of the energy loss is given by h_l and h_r alone. Independent of U, u_l and u_r the energy loss is equal in all reference frame translations. We are free to choose any inertial reference frame and choose the frame of reference in which $U = 0$. From (2.44) it follows that $u_r = -\alpha$. We are returning to the hydraulic jump! The energy loss

$$\begin{aligned} \frac{\alpha g}{4h_l}(h_l - h_r)^3 &= -\frac{u_r h_r g}{4h_r h_l}(h_l - h_r)^3 \\ &= -Q\frac{g(h_l - h_r)^3}{4h_r h_l} \end{aligned} \tag{2.46}$$

is identical to the classical energy loss of the hydraulic jump. The negative sign is due to the fact that this time the hydraulic jump is featured from right to left, opposite to the previous discussion in subsection (2.1.1). Further we see that $-u_r = \alpha > \sqrt{gh_r}$ if $h_l > h_r$ so u_r is supercritical conforming with the theory of the hydraulic jump.

2.6 Conclusions of the shallow water system

The shallow water model states that a bore will travel in a steady flow without the loss of mass nor momentum. It will however lose energy per time and width according to (2.45). A control volume around the discontinuity will contain the energy loss. The distance between the two cross-sections of this volume may become arbitrarily small. In the limit as the distance of the two cross-sections become zero the loss of energy needs to be instantaneous. The only physical effect to mimic this type of energy loss is turbulence. Thus the shallow water system postulates that all bores are turbulent.

Chapter 3

Favres experiments and the scientific debate on weak bores

In 1935 Favre published an extensive report of experiments on bores [8]. The experiments used a 75 meter long channel with a sink in one end and a source, in form of a pump, in the other end. In this way he maintained a flow of water of undisturbed depth and could superimpose a discharge on the flow, creating a discharge wave. By controlling the discharge of the pump Favre could create bores of variable bore heights.

Favres findings showed that the bore behaved qualitatively different depending on the bore strength. For $\frac{h_l}{hr} > 1.78$ the bore was turbulent as predicted by shallow water theory. If $1.28 < \frac{h_l}{hr} < 1.78$ a formation of undulations started to appear behind the bore front. Still the first undulations broke resulting in turbulence. For $\frac{h_l}{hr} < 1.28$ a train of undulations appeared behind the bore front none of which were breaking. These were the undular bores. These weak bores were without turbulence contrary to the predictions of the shallow water equations. This raised the question of how the undular bores were cooping with the classical energy loss found in the turbulent bores.

Lemoine [14] was the first to address the problem. He pointed out that the periodic waves observed behind the front of the weak bore somehow stored the energy that otherwise would dissipate through turbulence at the front of the bore. Further as Sturtevant puts it in [19]: "*Keulegan and Patterson suggested that these periodic waves were cnoidal waves, a type of non-linear dispersive wave. Benjamin and Lighthill(1954), investigating the problem further, showed that it is possible to patch a steady train of cnoidal waves downstream of a front to a uniform upstream flow only if there is a change at the front of either mass flux, momentum flux, or energy. If there were no change then the only possible steady wave would be a cnoidal wave of*

infinite wavelength, the solitary wave.“ According to the study of Benjamin and Lighthill a dissipation of about 20% of the classical energy loss is needed to explain the cnoidal wave-train behind the bore front. Finally Sturtevant complemented this study by showing that this predicted energy loss could well be dissipated through frictional effects at the bottom.

3.1 The dispersive systems and the KdV equation

In the shallow water system all surface displacement with $h'(x) < 0$ break. When confronted with Favres results on undular bores its therefore natural to wonder why the undulations behind the bore front do not break. The answer is that the weak bore does not follow the shallow water system. The shallow water system is founded on the assumption of long waves compared to the water depth, meaning no flow, and certainly no acceleration, in the vertical direction. As a result all waves in this system break. However as the wave is about to break the qualitative nature of the wave is changing. When the wave is almost discontinuous in the z-direction we can no longer neglect the acceleration of the water in this direction. To incorporate such effects dispersive systems were developed.

The predictions of shallow water theory that all waves in shallow water break were first challenged by Scott Russell(1844) who observed the solitary wave in shallow water. His observation was of a single stable hump of water travelling down a channel, with unaltered amplitude, for over a mile. The observation showed that a stable wave could exist in shallow water and led to a reform of shallow water theory.

The following derivation of the Boussinesq systems and the KdV equations is closely based on Whithams approach in [20]. Since we can no longer simply assume hydrostatic pressure, we need to formally explore surface waves. For this purpose it is convenient to express the flow by the velocity potential:

$$\phi_x = u, \quad \phi_z = w \tag{3.1}$$

This follows from our statement that water is irrotational $\nabla \times u = 0$. If we use the velocity potential in (1.1) we get the Laplace equation:

$$\phi_{xx} + \phi_{zz} = 0 \tag{3.2}$$

Lets assume an infinite channel with boundaries at the bottom and at the surface. The Laplace equation describes the motion of water limited only

by the boundary conditions. The water surface is defined by an interface between the water and the air. Let

$$f(x,z,t)=0 \tag{3.3}$$

describe this interface. No fluid may cross the interface. It follows that

$$\frac{Df}{Dt}=f_t+\phi_x f_x+\phi_z f_z=0 \tag{3.4}$$

Recall that $z=\eta(x,t)+H_0=h(x,t)$ at the surface. We define

$$f(x,z,t)\equiv h(x,t)-z.$$

From this we write

$$\frac{Dh}{Dt}=\eta_t+\phi_x\eta_x=\phi_z \tag{3.5}$$

This is the kinematic boundary condition of the surface. The pressure in the water is found by using (3.1) in (1.4) and (1.6) and integrating:

$$p-p_0=P(t)-\phi_t-\frac{1}{2}(\phi_x^2+\phi_z^2)-gz \tag{3.6}$$

This is known as Bernoullis equation, where p_0 is the pressure at the surface. It is common to absorb $P(t)$ into ϕ by letting $\phi'=\phi-\int P(t)dt$. However let us consider the point at infinity on the free surface; at such a point $\phi_t=u=w=h=0$, $z=H_0$ and $p=p_0$. Substituting this into (3.6) we have:

$$P(t)=gH_0.$$

From (3.6) with $P(t)$ as stated above we can deduce the dynamic boundary condition of the surface.

$$\phi_t+\tfrac{1}{2}(\phi_x^2+\phi_z^2)+g\eta=0 \quad \text{on} \quad z=h(x,t) \tag{3.7}$$

In addition we have the kinematic boundary condition at the bottom stating that no water is passing through the bottom.

$$\phi_z=0 \quad \text{on} \quad z=0 \tag{3.8}$$

Summarizing we have:

$$\begin{gathered}\phi_{xx}+\phi_{zz}=0, \quad 0<z<h(x,t)\\ \phi_z=0, \quad z=0\end{gathered}$$
$$\left.\begin{aligned}\eta_t+\phi_x\eta_x-\phi_z=0\\ \phi_t+\tfrac{1}{2}(\phi_x^2+\phi_z^2)+g\eta=0\end{aligned}\right\} z=h(x,t) \tag{3.9}$$

This is a general expression of surface waves in 2 dimensions. We now wish to incorporate shallow water conditions in a less radical way then above.

Previously we have claimed that, due to the shallow water, u, was uniform in any vertical cross-section. That is to say u is independent of z. Now the boundary condition at the bottom suggest that we expand the velocity potential as a power series:

$$\phi = \sum_{n=0}^{\infty} z^n f_n(x,t), \;\; f_1 = 0, \tag{3.10}$$

Substituting this expression for ϕ into the Laplace equation and equating the coefficients of z^n to zero, term by term, we arrive at the convergent series

$$\phi = f_0 - \frac{z^2}{2!}\frac{\partial^2 f_0}{\partial x^2} + \frac{z^4}{4!}\frac{\partial^4 f_0}{\partial x^4} - \frac{z^6}{6!}\frac{\partial^6 f_0}{\partial x^6}\cdots \tag{3.11}$$

Further more concerning the amplitude a of the surface waves we stated that the fraction now called $\alpha = \frac{a}{H_0}$ is of a small but not insignificant size. However α^2 is viewed as insignificant of size. On the wavelength of the surface waves we stated that the fraction now called $\beta = \frac{H_0^2}{\lambda^2}$ was insignificant. That is to say that the wavelength was a lot bigger then the depth of the undisturbed water. However due to the wave steepening close to wave breaking we now modify this assumption and treat β as a significant number, however hold any term of β^2 to be insignificant of size. In order to illuminate the size of the terms in (3.9) we normalize the variables by taking the original variables (primed) to be

$$x' = \lambda x, \quad z' = H_0 z, \quad t' = \frac{\lambda t}{c_0}$$

$$\eta' = a\eta, \quad \phi' = \frac{g\lambda a\phi}{c_0}.$$

In this way we can formulate (3.9) as

$$\begin{gathered} \beta\phi_{xx} + \phi_{zz} = 0, \quad 0 < z < 1 + \alpha\eta \\ \phi_z = 0, \quad z = 0 \\ \left.\begin{aligned} \eta_t + \alpha\phi_x\eta_x - \tfrac{1}{\beta}\phi_z = 0 \\ \phi_t + \tfrac{1}{2}(\alpha\phi_x^2 + \tfrac{\alpha}{\beta}\phi_z^2) + \eta = 0 \end{aligned}\right\} z = 1 + \alpha\eta \end{gathered} \tag{3.12}$$

And (3.11) as

$$\phi = \sum_{n=0}^{\infty}(-1)^m \frac{z^{2m}}{(2m)!}\beta^m \frac{\partial^{2m} f_0}{\partial x^{2m}} \tag{3.13}$$

Substituting this into the surface conditions in (3.12) we get:

$$\begin{aligned}\eta_t + \{(1+\alpha\eta)\, f_x\}_x - \left\{\tfrac{1}{6}(1+\alpha\eta)^3 f_{xxxx} + \tfrac{1}{2}\alpha(1+\alpha\eta)^2 \eta_x f_{xxx}\right\}\beta + O(\beta^2) = 0 \\ \eta + f_t + \tfrac{1}{2}\alpha f_x^2 - \tfrac{1}{2}(1+\alpha\eta)^2\left\{f_{xxt} + \alpha f_x f_{xxx} - \alpha f_{xx}^2\right\}\beta + O(\beta^2) = 0\end{aligned} \tag{3.14}$$

Please note from the derivative of (3.11) with respect to x that f_x is u to the first order and is exactly u at the bottom. Since we are not using the y dimension we borrow the variable v. Let $v = f_x$.

In reaching the expressions above all terms of order β^2 are neglected. If we discard the β terms all together we have that $u = f_x$ and by substitution we see that we get the shallow water equations (2.9) normalized. As stated above we are keeping the β terms but since α and β are small we are neglecting any terms of order $\alpha\beta$. Neglecting terms of order $\alpha\beta$ and taking the derivative of the second equation with respect to x gives

$$\begin{aligned}\eta_t + \{(1+\alpha\eta)\, v\}_x - \tfrac{1}{6}\beta v_{xxx} + O(\alpha\beta, \beta^2) = 0 \\ v_t + \alpha v v_x + \eta_x - \tfrac{1}{2}(\beta) v_{xxt} + O(\alpha\beta, \beta^2) = 0\end{aligned} \tag{3.15}$$

These are a variant of the Boussinesq's equations. To the same order of accuracy we have

$$\phi_x = v - \beta\frac{z^2}{2} v_{xx} + O(\beta^2). \tag{3.16}$$

Averaging the value over the normalized depth gives

$$\tilde{u} = v - \frac{1}{6}\beta v_{xx} + O(\alpha\beta, \beta^2); \tag{3.17}$$

expressed in terms of v

$$v = \tilde{u} + \frac{1}{6}\beta \tilde{u}_{xx} + O(\alpha\beta, \beta^2). \tag{3.18}$$

We apply this to (3.15)

$$\begin{aligned}\eta_t + \{(1+\alpha\eta)\tilde{u}\}_x + O(\alpha\beta, \beta^2) = 0 \\ \tilde{u}_t + \alpha\tilde{u}\tilde{u}_x + \eta_x - \tfrac{1}{3}(\beta)\tilde{u}_{xxt} + O(\alpha\beta, \beta^2) = 0\end{aligned} \tag{3.19}$$

This is a system of equations equivalent to (2.9) but with an extra term $-\frac{1}{3}(\beta)\tilde{u}_{xxt}$ expressing the effect of the vertical acceleration on the pressure. We will discuss this difference later.

The Korteweg-de Vries equation is derived from any of these systems by specializing to a wave moving to the right. To lowest order, neglecting terms of order α and β, such a solution of (3.15) has

$$v = \eta,\ \eta_t + \eta_x = 0.$$

We look for a solution, corrected to first order in α and β, in the form

$$v = \eta + \alpha A + \beta B + O(\alpha^2, \beta^2),$$

where A and B are functions of η and its x derivatives. Then equations (3.15) become

$$\begin{aligned} \eta_t + \eta_x + \alpha(A_x + 2\eta\eta_x) + \beta(B_x - \tfrac{1}{6}\eta_{xxx}) + O(\alpha^2, \beta^2) = 0 \\ \eta_t + \eta_x + \alpha(A_t + \eta\eta_x) + \beta(B_t - \tfrac{1}{2}\eta_{xxt}) + O(\alpha^2, \beta^2) = 0 \end{aligned} \tag{3.20}$$

Since $\eta_t = -\eta_x + O(\alpha, \beta)$, all t derivatives in the first order terms may be replaced by minus the x derivatives. The two equations are consistent if

$$A = -\frac{1}{4}\eta^2, \; B = \frac{1}{3}\eta_{xx}$$

Hence we have

$$\begin{aligned} v = \eta - \tfrac{1}{4}\alpha\eta^2 + \tfrac{1}{3}\beta\eta_{xx} + O(\alpha^2, \beta^2) \\ \eta_t + \eta_x + \tfrac{3}{2}\alpha\eta\eta_x + \tfrac{1}{6}\beta\eta_{xxx} + O(\alpha^2, \beta^2) = 0. \end{aligned} \tag{3.21}$$

The second equation is the normalized form of the Korteweg-de Vries equation. Returning to original variables the KdV equation becomes

$$\eta_t + c_0\left(1 + \frac{3}{2}\frac{\eta}{H_0}\right)\eta_x + \frac{1}{6}c_0 H_0^2 \eta_{xxx} + O(\alpha^2, \beta^2) = 0. \tag{3.22}$$

3.2 Surface wave solutions

To check if this equation has solutions that do not break we search for travelling solutions to η on the form:

$$\eta = H_0\zeta(\xi), \quad \xi = x - Ut. \tag{3.23}$$

Where U is the travelling speed of the solution corresponding to the shock speed for the shallow water system. Assuming a solution on this form the partial differential equation (3.22) turns into an ordinary differential equation

$$\frac{1}{6}H_0^2\zeta''' + \frac{3}{2}\zeta\zeta' - \left(\frac{U}{c_0} - 1\right)\zeta' = 0.$$

Which integrates to

$$\frac{1}{6}H_0^2\zeta'' + \frac{3}{4}\zeta^2 - \left(\frac{U}{c_0} - 1\right)\zeta + G = 0.$$

Multiplying this by ζ' and integrating again we obtain

$$\frac{1}{3}H_0^2\left(\frac{d\zeta}{d\xi}\right)^2+\zeta^3-2\left(\frac{U}{c_0}-1\right)\zeta^2+4G\zeta+H=0 \tag{3.24}$$

where G and H are constants of integration. In the special case when ζ and its derivatives tend to zero at ∞, $G=H=0$, (3.24) simplifies to

$$\begin{gathered}\tfrac{1}{3}H_0^2\left(\tfrac{d\zeta}{d\xi}\right)^2=\zeta^2\left(\alpha-\zeta\right),\\ \tfrac{U}{c_0}=1+\tfrac{\alpha}{2}.\end{gathered} \tag{3.25}$$

Since $\zeta=0$ at $\xi=\infty$ it follows that ζ rises from $\zeta=0$ to a maximum $\zeta=\alpha$ before symmetrically sinking to $\zeta=0$ at $\xi=-\infty$. This is the solitary wave. From this we see that the range of η is $\eta_0=H_0\alpha$ showing that α plays the same role as in deriving the KdV equation. The velocity of the solitary wave is

$$U=c_0\left(1+\frac{1}{2}\frac{\eta_0}{H_0}\right) \tag{3.26}$$

And the solution to (3.25) is

$$\zeta=\alpha\mathrm{sech}^2\left(\frac{3\alpha}{4H_0^2}\right)^{\frac{1}{2}}\xi \tag{3.27}$$

which can be checked by inserting into (3.25). Written in terms of η it becomes

$$\eta=\eta_0\mathrm{sech}^2\left\{\left(\frac{3\eta_0}{4H_0^3}\right)^{\frac{1}{2}}(x-Ut)\right\}. \tag{3.28}$$

This is a solitary wave travelling at the speed U. It appears to apply for all heights, but this is not true as the KdV equation which this is a solution to is derived under the assumption that α is small.

More generally equation (3.24) describes the wave profile of the steady wave. Rewritten as

$$\frac{1}{3}H_0^2\left(\frac{d\zeta}{d\xi}\right)^2=-\zeta^3+2\left(\frac{U}{c_0}-1\right)\zeta^2-4G\zeta-H \tag{3.29}$$

the equation states that the squared change of the surface with ξ is given by a cubic polynomial of the surface. A cubic polynomial has 4 degrees of freedom. Thereby it is given by its 3 zeros and the amplitude that connects them. Factorized it becomes

$$p_3(\zeta)=a_0(\zeta-\zeta_1)(\zeta-\zeta_2)(\zeta-\zeta_3)$$

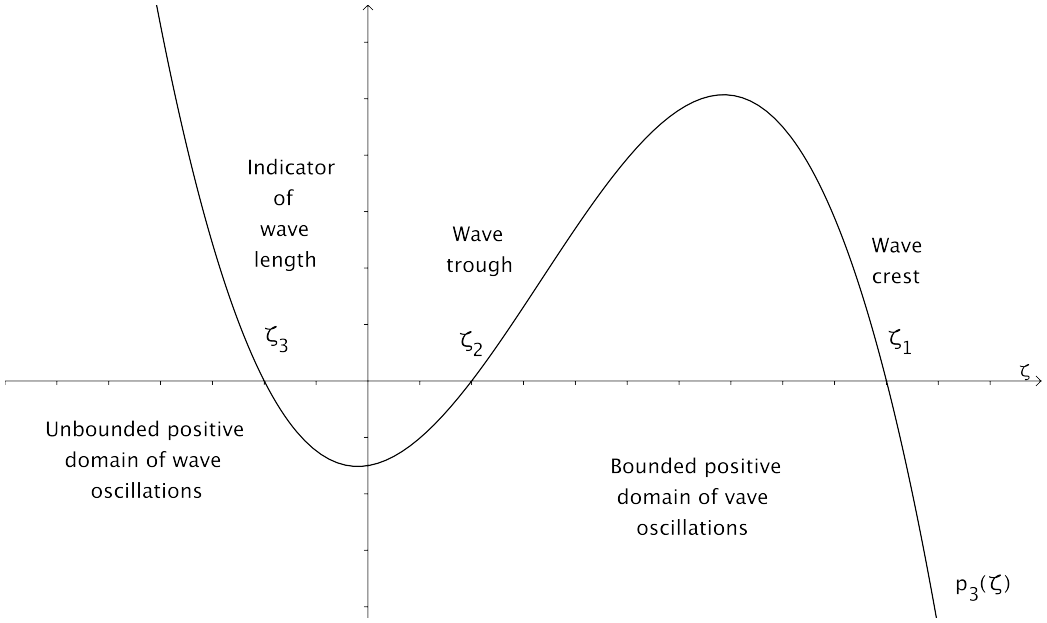

Figure 3.1: The figure is showing a cubic $p_3(\zeta)$. Since $\left(\frac{d\zeta}{d\xi}\right)^2 = p_3(\zeta)$, we are interested in domains of ζ where $p_3(\zeta) > 0$. In this figure $p_3(\zeta)$ has three real and unique points of zero. This gives two domains of ζ where the cubic is positive. Only the domain $[\zeta_2, \zeta_1]$ gives bounded values for $p_3(\zeta)$. The smallest value ζ_2 gives the wave trough and the largest value ζ_1 gives the wave crest.

where a_0 is the connecting amplitude. The surface wave can also be said to have 4 degrees of freedom. Its minimum and maximum amplitude, its wave length and its frequency. By introducing steady flow through the parameter ξ, we have set the frequency of the surface waves to zero, but the minimum and maximum amplitude and the wave length are still undetermined. The cubic on the right hand side of (3.29) from which these are to be determined has three degrees of freedom as the sign of ζ^3 is given as negative.

Assume that the cubic in (3.29) has 3 zeros that are real and unique as given in figure 3.1. The change of the surface with ξ is squared and only real changes of the surface are meaningful. This means that only values of ζ where the cubic is positive are allowed. Two such domains exist $\zeta \in [-\infty, \zeta_3]$ and $\zeta \in [\zeta_2, \zeta_1]$. The first domain is discarded as unbound values of ζ are meaningless. We conclude that the two zeros ζ_2 and ζ_1 represent the minimum and maximum value of ζ respectively. The wave length is determined by a relation between ζ_1, ζ_2 and ζ_3.

Let $\zeta(\xi_2) = \zeta_2$ and $\zeta(\xi_1) = \zeta_1$. The wave length is two times the distance from the wave‘s minimum to the wave‘s maximum.

$$\lambda = 2\int_{\xi_2}^{\xi_1} d\xi \tag{3.30}$$

By separation of (3.29) we have that

$$2\int_{\xi_2}^{\xi_1} d\xi = \frac{2H_0}{\sqrt{3}} \int_{\zeta_2}^{\zeta_1} \frac{d\zeta}{[(\zeta_1-\zeta)(\zeta-\zeta_2)(\zeta-\zeta_3)]^{\frac{1}{2}}} \tag{3.31}$$

Here we use the substitution

$$\begin{aligned} \zeta &= \zeta_2 + (\zeta_1-\zeta_2)\sin^2\theta = \zeta_1 - (\zeta_1-\zeta_2)\cos^2\theta \\ dz &= 2(\zeta_1-\zeta_2)\cos\theta\sin\theta d\theta \end{aligned} \tag{3.32}$$

which gives the following expression for the wave length

$$\begin{aligned} \lambda &= \tfrac{4H_0}{\sqrt{3}} \int_0^{\frac{\pi}{2}} \frac{(\zeta_1-\zeta_2)\cos\theta\sin\theta d\theta}{\left[(\zeta_1-\zeta_2)\sin^2\theta(\zeta_1-\zeta_2)\cos^2(\zeta_1-\zeta_3-(\zeta_1-\zeta_2)\cos^2\theta)\right]^{\frac{1}{2}}} \\ &= \tfrac{4H_0}{\sqrt{3(\zeta_1-\zeta_3)}} \int_0^{\frac{\pi}{2}} \frac{d\theta}{\left[1-k^2\sin^2\theta\right]^{\frac{1}{2}}} = \tfrac{4H_0}{\sqrt{3(\zeta_1-\zeta_3)}} K(k) \end{aligned} \tag{3.33}$$

where

$$K(k) = \int_0^{\frac{\pi}{2}} \frac{d\theta}{\left[1-k^2\sin^2\theta\right]^{\frac{1}{2}}} \tag{3.34}$$

is the complete elliptic integral of the first kind with modulus $k = \left[\frac{\zeta_1-\zeta_2}{\zeta_1-\zeta_3}\right]^{\frac{1}{2}}$.

From what we have deduced so far it is obvious that we need 3 real zeros of $p_3(\zeta)$ to possibly have a surface. If 2 zeros are complex the surface will be unbounded. However the restriction that the zeros needed to be unique can be relaxed. If $\zeta_1 = \zeta_2$ we get that the maximum and minimum value of the wave are equal, that is waves with zero amplitude. The question of wave length of such waves is redundant. If $\zeta_2 = \zeta_3$ we have that $k^2 = 1$. It is possible to show that

$$K(k) \sim \frac{1}{2} \log \left\{ 16/(1-k^2) \right\} \tag{3.35}$$

as $k^2 \to 1^-$ and so $K(k) \to +\infty$ as $k^2 \to 1^-$. It follows that as $\zeta_3 \to \zeta_2$ the wave length becomes infinite $\lambda \to +\infty$. We conclude that if the zeros coincide we either have no waves or as in the special case above the solitary waves.

3.3 Cnoidal waves

The integral

$$v = \int_0^{\phi} \frac{d\theta}{\left[(1 - k^2 \sin^2(\theta) \right]^{\frac{1}{2}}} \tag{3.36}$$

is an elliptic integral. It differs from the complete elliptic integral in that it has variable limits of integration. In connection with this integral Jacobi and also Abel defined a new pair of inverse functions

$$\mathrm{sn}(v|k^2) = \sin\phi, \quad \mathrm{cn}(v, |k^2) = \cos\phi \tag{3.37}$$

which are two of the Jacobian elliptic functions. In the two special cases where $k^2 \in \{0, 1\}$ the integral (3.36) gives $v = \phi$ and $v = \mathrm{arcsech}(\cos\phi)$. For these cases the Jacobian elliptic function $\mathrm{cn}(v|k^2)$ become

$$\begin{array}{ll} v = \phi, & \mathrm{cn}(v|0) = \cos\phi = \cos v, \\ v = \mathrm{arcsech}(\cos\phi), & \mathrm{cn}(v|1) = \mathrm{sech} v. \end{array} \tag{3.38}$$

The elliptic function $\mathrm{cn}(v, |k^2)$ is a periodic function for $0 \leq k^2 < 1$ where as at $k^2 = 1$ the periodicity is lost as the period becomes infinite.

When developing the cnoidal wave solution to (3.24) we use the Jacobian elliptic function $\mathrm{cn}(v, |k^2)$, hence the name cnoidal wave. The development follows the same procedure as for the wave length, but with different limits of integration. Implicitly solved the solution to (3.24) is

$$\xi = \xi_2 \pm \frac{2H_0}{\sqrt{3}} \int_{\zeta_2}^{f} \frac{d\zeta}{\left[(\zeta_1 - \zeta)(\zeta - \zeta_2)(\zeta - \zeta_3) \right]^{\frac{1}{2}}} \tag{3.39}$$

where the top limit $f(\xi)$ is the cnoidal wave solution. We use the substitution (3.32) to transform this integral into a standard elliptic integral as before

$$\xi = \xi_2 \pm \frac{4H_0}{\sqrt{3(\zeta_1 - \zeta_3)}} \int_0^{\phi} \frac{d\theta}{\left[(1 - k^2 \sin^2(\theta)\right]^{\frac{1}{2}}}. \tag{3.40}$$

It follows from (3.32) that the wave solution is given as

$$f = \zeta_2 + (\zeta_1 - \zeta_2) \sin^2 \phi = \zeta_1 - (\zeta_1 - \zeta_2) \cos^2 \phi. \tag{3.41}$$

Using the definition of the Jacobian elliptic function $\mathrm{cn}(v|k^2)$ in (3.38) we have that

$$\mathrm{cn}\left[(\xi - \xi_2)\left\{\sqrt{3(\zeta_1 - \zeta_3)}/4H_0\right\}|k^2\right] = \cos\phi, \tag{3.42}$$

where the $\pm$ is suppressed since cn is an even function. Based on this we get

$$f(\xi) = \zeta_1 - (\zeta_1 - \zeta_2)\mathrm{cn}^2\left[(\xi - \xi_2)\left\{\sqrt{3(\zeta_1 - \zeta_3)}/4H_0\right\}|k^2\right] \tag{3.43}$$

the cnoidal wave solution.

From this solution we see that the spectre of wave forms called cnoidal waves is quite large. The special cases when $k^2 \in \{0, 1\}$ gives the sinusoidal wave form for $k^2 = 0$ and solitary wave form for $k^2 = 1$ and thus both sinusoidal and solitary waves are cnoidal waves. In this thesis however we treat these special cases as individual wave forms and differentiate them from the wave forms found when the modulus is between 0 and 1. For further reading on cnoidal waves [7] can be recommended.

Chapter 4

Benjamin and Lighthill

In the previous section we derived the KdV equation (3.22). Assuming steady solutions, (3.22) could be written as (3.24) which was satisfied both by solitary and more generally cnoidal waves. However (3.24) contains constants of integration that lack explanation. Benjamin and Lighthill present the same equation in a way that illuminates these constants. Their first assumption is steady flow. By steady flow we mean that (1.4) and (1.6) has solutions of the form $u(x,z,t) = u(x-Ut,z)$ and $w(x,z,t) = w(x-Ut,z)$. [1] That is travelling wave solutions where U is the travelling speed. To see that this is steady flow we go to a reference frame travelling at the same speed. If the initial solutions be marked u' and w' then in this new reference frame $u = u' - U$ and $w = w'$. Applying this to (1.4) and (1.6) we get

$$\begin{aligned} u_t + Uu_x + uu_x + wu_z &= \tfrac{-p_x}{\rho} \\ w_t + Uw_x + uw_x + ww_z &= \tfrac{-p_z}{\rho} - g. \end{aligned} \tag{4.1}$$

Since $u_t = -Uu_x$ and $w_t = -Uw_x$ this simplifies to

$$\begin{aligned} uu_x + wu_z &= \tfrac{-p_x}{\rho} \\ uw_x + ww_z &= \tfrac{-p_z}{\rho} - g. \end{aligned} \tag{4.2}$$

the time independent Euler equations of two dimensions. Now we introduce the stream function. It applies to two dimensional flow and its definition, $\psi_y \equiv u$ and $-\psi_x \equiv w$, is designed to satisfy the continuity equation (1.1) for an incompressible fluid. In addition the stream function gives the volume rate of flow between two streamlines. Thus defining it to be zero at the bottom, the stream function is Q at the surface where Q is the volume rate of flow of the fluid. Finally since the flow is irrotational ψ satisfies the Laplace

[1] Note that we still regard $v = 0$.

equation. Inserting ψ in (4.2) and integrating we get

$$\frac{1}{2}\psi_x^2 + \frac{1}{2}\psi_y^2 + gz = -\frac{p}{\rho} + R \tag{4.3}$$

as in (3.6) but without time dependence. Here p is measured relative to the atmospheric pressure. Thus at the surface we have:

$$\frac{1}{2}\psi_x^2 + \frac{1}{2}\psi_y^2 + gh = R.$$

Where R is constant for all cross-sections of the flow. Benjamin and Lighthill states further that in order to have time-independent flow the total moment flux S needs to be independent of the cross-section. The moment flux in a cross-section is given by:

$$S = \int_0^h (\frac{p}{\rho} + \psi_z^2)dy = \int_0^h [R - gy - \frac{1}{2}\psi_x^2 + \frac{1}{2}\psi_y^2]dy \tag{4.4}$$

The second integral is reached by replacing $\frac{1}{2}\psi_y^2$ in the first integral with its equivalent from (4.3). Now Benjamin and Lighthill makes an assumption on how the stream function can be expanded as a series in much the same way as we did with the velocity potential in deriving the KdV equation.

$$\psi = zf(x) - \frac{z^3}{3!}f''(x) + \frac{z^5}{5!}f^{(IV)}(x) - \cdots \tag{4.5}$$

Using this series in the second integral of (4.4) neglecting terms of order z^4 we get

$$S = Rh - \frac{1}{2}gh^2 - \frac{1}{6}h^3(f')^2 + \frac{1}{2}hf^2 - \frac{1}{6}h^3ff'' \tag{4.6}$$

We know that at $\psi = Q$ at $z = h$. Still neglecting terms of order z^4 this gives us:

$$Q = hf(x) - \frac{h^3}{6}f''(x).$$

Written as an expression for $f(x)$ we have

$$f(x) = \frac{Q}{h} + \frac{1}{6}h^2f''(x) \tag{4.7}$$

Using this in (4.6) we get:

$$\begin{aligned}
\frac{1}{6}h^3f'^2 &= \frac{1}{6}\frac{Q^2}{h}h'^2 + O(h'^2h^2, h'h^3, h^4) \\
\frac{1}{2}hf^2 &= \frac{1}{2}\frac{Q^2}{h} + \frac{1}{6}Qh^2f'' + O(h^4) \\
\frac{1}{6}h^3ff'' &= \frac{1}{6}Qh^2f'' + O(h^4)
\end{aligned}$$

And (4.6) becomes

$$S = Rh - \frac{1}{2}gh^2 - \frac{1}{6}\frac{Q^2}{h}h'^2 + \frac{1}{2}\frac{Q^2}{h} + O(h'^2h^2, h'h^3, h^4) \tag{4.8}$$

Rearranging it we get

$$\frac{1}{3}Q^2(\frac{dh}{dx})^2 + gh^3 - 2Rh^2 + 2Sh - Q^2 = 0 \tag{4.9}$$

We see that this equation is equivalent to (3.24) but the meaning of the constants are much clearer. Q is the volume flow per unit span; R is the energy per unit mass; and S is the momentum flow rate per unit span. In the absence of friction these values are constant, at every cross-section of a steady flow. For a uniform stream of speed u_1 and depth h_1, Q, R and S take the values

$$Q_1 = u_1h_1, \quad R_1 = \tfrac{1}{2}u_1^2 + gh, \quad S_1 = u_1^2h_1 + \tfrac{1}{2}gh_1^2. \tag{4.10}$$

From our equation (4.9) we see that Q, R and S determines the stationary waves completely. For the undular bore the condition given in (4.10) must hold upstream[2] of the bore front, see region 1 in figure 4.1. Since Q, R and S are constant in a frictionless flow we apply (4.10) in (4.9) factorizing the cubic in (4.9) to

$$(h - h_1)^2(gh - v_1^2) \tag{4.11}$$

This is a case of coincident roots which we learnt means that we either have no waves or a solitary wave. Either we have $v_1^2 < gh_1$ which is subcritical flow and no bore condition at all. Or the supercritical flow $v_1^2 > gh_1$ corresponding to a solitary wave. We see further that a train of cnoidal waves is attainable if R in the cubic is reduced. This leads to a solution with three simple roots. The conclusion of Benjamin and Lighthill is simple. In order to get Favres observed cnoidal waves a reduction of R, that is a small amount of dissipation, is needed.

4.1 Sturtevant

Sturtevant goes one step further in his paper [19] as he aims to show by what means the energy is dissipated. The first step is to normalize (4.9) reached by Benjamin and Lighthill. Let $w = \frac{h}{h_1}$ be the non-dimensional depth and

[2] In figure 4.1 region 1 appears to be downstream but in bore fixed coordinates all fluid move to the right and region 1 is upstream.

$z = \frac{x}{h_1}$ be the horizontal coordinate, where h_1 is undisturbed depth. We then need to normalize Q, R and S. For a uniform stream we have at some cross-section

$$Q_1 = u_1 h_1, \quad R_1 = \tfrac{1}{2}u_1^2 + gh_1, \quad S_1 = u_1^2 h_1 + \tfrac{1}{2}gh_1^2 \tag{4.12}$$

The flow speed u_1 is normalized by $c_1 = \sqrt{(gh_1)}$, the speed of travelling waves on undisturbed water. The mass flow, energy and momentum flux Q, R and S take values close to those of Q_1, R_1 and S_1 leading to

$$q = \frac{Q}{c_1 h_1}, \quad r = \frac{2R}{3c_1^2}, \quad S = \frac{2S}{3c_1^2 h_1} \tag{4.13}$$

as their normalization. Step by step the normalization of (4.9) is

$$\begin{aligned} \frac{1}{3}q^2 (c_1 h_1)^2 \left(\frac{dh}{dx}\right)^2 + gh^3 - 3rc_1^2 h^2 + 3sc_1^2 h_1 h - q^2 (c_1 h_1)^2 = 0 \\ \frac{1}{3}q^2 h_1^3 \left(\frac{dh}{dx}\right)^2 + h^3 - 3rh_1 h^2 + 3sh_1^2 h - q^2 h_1^3 = 0 \\ \frac{1}{3}q^2 \left(\frac{dw}{dz}\right)^2 + w^3 - 3rw^2 + 3sw - q^2 = 0 \end{aligned} \tag{4.14}$$

The advantage of this normalization compared to the one chosen by Benjamin and Lighthill in their paper, is that it makes the fluid volume flow explicit.

The cubic in (4.14)

$$w^3 - 3rw^2 + 3sw - q^2 = 0 \tag{4.15}$$

may have the zeros w_1, w_2, and w_3 where, as before, the first two zeros are the depth under the crest and through of the cnoidal waves and the last zero indicates the wavelength by the relation, given by Sturtevant,

$$\Lambda = \frac{\lambda}{h_1} = 4\left[\frac{w_1 w_2}{3}\left(\frac{w_1}{w_1 - w_2}k^2 - 1\right)\right]^{\frac{1}{2}} K(k) \tag{4.16}$$

where $K(k)$ is the complete elliptic integral of the first kind with modulus $k = [(w_1 - w_2)/(w_1 - w_3)]^{\frac{1}{2}}$. Given w_1, w_2 and Λ, (4.16) gives k, or w_3. Once we found the zeros of (4.15) we can factorize it giving

$$w^3 - 3rw^2 + 3sw - q^2 = (w - w_1)(w - w_2)(w - w_3) \tag{4.17}$$

From this we see that

$$\begin{aligned} (w - w_1)(w - w_2)(w - w_3) \\ = w^3 - w^2(w_1 + w_2 + w_3) + w(w_1 w_2 + w_2 w_3 + w_1 w_3) - w_1 w_2 w_3 \end{aligned} \tag{4.18}$$

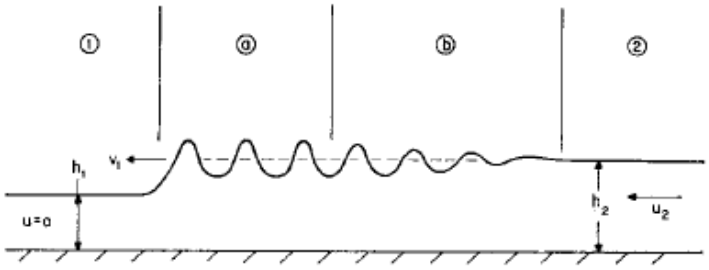

Figure 4.1: Figure from Sturtevants paper [19]: This figure displays the undular bore in 4 regions. Region 1 is the undisturbed water depth of the channel. Region a shows the stable part of the oscillation at the front. Region b shows the unstable part of the bore where new waves are continuously created. Finally region 2 is the sum of undisturbed water and extra discharge released by the pump i.e. the potential from where the bore originate. The figure is in channel fixed coordinates where the bore speed v is to the left.

And comparing this with the first form of the cubic reveals

$$q^2 = w_1 w_2 w_3, \quad 3r = w_1 + w_2 + w_3, \quad 3s = w_1 w_2 + w_2 w_3 + w_1 w_3. \tag{4.19}$$

It follows that from experimental data measuring the depth under the wave crest and through and the wave length it is possible to calculate the mass flux, momentum flux and energy of the flow in the region of the cnoidal waves. These measurements are found in six of Favres runs. Before looking at the specific calculations we review Sturtevants arguments.

When considering a bore Sturtevant divides it into 4 regions as shown in figure 4.1. Region 1 is ahead of the bore front. This region is obviously steady as the flow velocity, using channel fixed coordinates, is $u_1 = 0$ in this region. At the bore front we have region a. This region is also said to be steady as it is assumed to contain a wave train of cnoidal waves developed as the bore has travelled down the channel. The steady solutions travel at the bore velocity and thus we use a reference frame travelling with the bore front. Behind region a is the unsteady region b where new waves continually form and grow until they have developed into the cnoidal waves of region a. At the end is region 2 which is the potential from which the cnoidal waves grow out of. In Favres experiment this is the extra water being continually pumped into the channel. Sturtevant writes: "*As the bore propagates down the channel, waves continually form behind it, region a grows, and region b moves downstream relative to the front. Presumably, a long time after generating the bore, the flow downstream of the front consists of an infinite train of stationary waves.*".

Since the flow is steady in region 1 and region a, q is constant at every cross section of these regions. But we can evaluate momentum and energy loss through the bore front by comparing s_1 with s and r_1 with r. The measurements in Favres six runs are given in table (4.1) and the results of Sturtevants calculations are given in table (4.2). The tables presented contains some corrections of minor calculation errors done by Sturtevant, however these errors in no way changes the conclusion drawn by the results. It is worth noting that Favre measured the wave lengths with one decimals accuracy, and the extra decimals presented by Sturtevant and here are unfounded however this lack of accuracy does not effect the calculations of energy and momentum.

Table 4.1: Favres measurements: This tables present the measurements done by Favre in run 21-24, 26 and 29. The values h_1 and h_2 are given in decimetre and are the depths of region one and two in figure (4.1) respectively. The values w_1 and w_2 are the normalized depths under the crest and trough of the undulations found behind the bore front as shown in region a of figure (4.1). Λ is the normalized wavelength of these waves. The normalization used is the undisturbed depth given by h_1.

Run no	h_1	h_2	w_1	w_2	Λ
21	1.078	1.164	1.108	1.020	11.309
22	1.073	1.223	1.259	1.050	9.413
23	1.079	1.327	1.443	1.029	8.434
24	1.074	1.376	1.560	1.031	8.007
26	1.075	1.478	1.603	1.250	5.860
29	1.061	1.592	1.635	1.465	5.090

The first step in these calculations is to find k^2, the rest follow from this. The k^2 is calculated from (4.16).

$$\Lambda = 4\left[\frac{w_1 w_2}{3}\left(\frac{w_1}{w_1 - w_2}k^2 - 1\right)\right]^{\frac{1}{2}} K(k)$$

Rewritten to solve for k^2 implicitly we have:

$$k^2 = \left[\left(\frac{\Lambda}{4K(k)}\right)^2 \frac{3}{w_1 w_2} + 1\right]\left(\frac{w_1 - w_2}{w_1}\right) \tag{4.20}$$

This expression is not solved analytically. But using built in Matlab codes like quad for the elliptic integral and fzero to solve (4.20), solutions to k^2

Table 4.2: Sturtevants calculations: This table display the values calculated from Favres measurements as described in this section. Of these results the values $\frac{r}{r_1}$ and $\frac{s}{s_1}$ are most important. These values are always greater then one and this indicates that the fluid is gaining energy as it, in bore fixed coordinates, passes from region 1 to region a completely contrary to what we would believe.

Run no	k^2	w_3	$q = F_1$	$\frac{r}{r_1}$	$\frac{s}{s_1}$	$\frac{r-r_2}{r_1-r_2}$
21	0.5325	0.9427	1.032	1.0017	1.0017	23.5
22	0.6704	0.9472	1.119	1.0012	1.0014	4.4
23	0.7964	0.9232	1.171	1.0072	1.0068	5.9
24	0.8181	0.9134	1.212	1.0102	1.0094	5.1
26	0.4376	0.7963	1.263	1.0149	1.0201	3.8
29	0.1813	0.6973	1.292	1.0346	1.0499	4.0

are easily obtained. Once we have a value of k^2 we calculate w_3 from the modulus relation $k^2 = (w_1 - w_2)/(w_1 - w_3)$. We get q, r and s from (4.19). While the values

$$q_1 = q = F_1, \quad r_1 = \tfrac{1}{3}F_1^2 + \tfrac{2}{3}, \quad s_1 = \tfrac{2}{3}F_1^2 + \tfrac{1}{3} \tag{4.21}$$

follow from the normalization. To calculate r_2, in the last column of table (4.2) we use the difference $r_1 - r_2$ which expresses the classical energy loss for any volume of fluid having passed through the bore front

$$r_1 - r_2 = \frac{g(h_2 - h_1)^3}{4h_1h_2}. \tag{4.22}$$

The results of Sturtevants calculations are at first very surprising. Since $\frac{r}{r_1} > 1$ in all runs there is not a loss but a gain of energy through the bore front in contrary to the classical theory. Sturtevants explanation is that the boundary lair must influence the bore. Following the bore in figure 4.1 in bore fixed coordinates we see that in region 1 the boundary has no influence on the fluid as both the boundary and the fluid are moving with the same speed. The same is not case for region a where the boundary obviously moves to the right faster then the fluid, presumably adding energy and momentum to the fluid in this region. This explains why the fluid in region a has gained energy rather then lost it. Finally the last column of table 4.2 shows that the energy added by the boundary are in all cases several times the classical energy loss indicating that the boundary plays a vital role.

4.2 Conclusion of Benjamin and Lighthill and Sturtevant

Summing up the reasoning of Benjamin and Lighthill, they showed that for any steady flow in shallow water the range of possible surface waves is the full spectre of cnoidal waves from sinusoidal to solitary waves. Further they showed that the type of surface waves encountered was dependent on the conservation of mass, energy and momentum. If all three are conserved the only possible surface waves are solitary waves. Only a loss of energy or increase in momentum, loss of mass being unacceptable, would give oscillating periodic surface waves. The undular bores were observed to have oscillating waves of a cnoidal character. This lead to the conclusion that the undular bore somehow dissipates some energy. Sturtevant followed up this train of thought by calculating the energy loss through the bore front. He found an energy gain. And he presented frictional effects at the bottom as the only possible explanation for this result. However both these lines of reasoning hinge on the idea that the bore obtains a steady flow which as Alfatih and Kalisch puts it neglects dynamical effects.

Chapter 5

Three lines of argument that challenge the views of Benjamin and Lighthill and Sturtevant.

We must be aware that there are two issues under discussion. One concerns the dispersive model of the undular bore. The other concerns the undular bore itself. The dispersive model of the undular bore and the undular bore itself are not the same. It is not possible to make statements of the bore itself from the model of the bore unless the model of the bore and the bore itself coincide. Also any statement made on the basis of the model can not go beyond the reach of the model. It is however possible, by comparing experimental data on the bore itself and simulated data by the model, to make statements about the bore models accuracy. These principles seems not to be upheld by Sturtevant. The claim that the bore experiences dissipation through friction at the boundary lair is based upon calculations using a model in which the fluid is in-viscous. Such a claim must then be viewed with suspicion. Further Benjamin and Lighthills analysis is founded on the assumption that the bore quickly establishes a steady flow at the front. This assumption is based on Keulegan and Pattersons calculations of the experimental data recorded by Favre, where the travelling speed of the waves were found close to those of cnoidal waves. But even Keulegan and Patterson have reservations on the results and suggest further experiments. No argument is put forward, to suggest, that the dispersive model used has such steady solutions to the undular bore. In other words: Even if the experimental data suggest that the flow is steady, this does by no means guarantee that the dispersive model gives a steady flow. This can only be determined by a numerical treatment of the KdV equation or an equivalent dispersive system.

From a physical point of view steady flow is connected with a balance

of forces. Expressions of steady flow typically appears in channels of slight tilts were the effects of gravity and friction are cancelled out. Friction plays an integral part in the concept of steady flow and a model without friction might have problems establishing such a flow. When modelling a bore it is common to use

$$\eta(x,0) = \frac{1}{2}a_0[1 - \tanh(kx)]$$

as an initial value for the surface. Here η is the deviation from the undisturbed depth. This initial profile is the smooth equivalent of the shock solution in classical shallow water theory. In the case of the KdV equation this initial profile is rapidly changing, attaining a profile of undulations behind the bore front, which suggests that at least initially it is not steady. When does it become steady? This question has been neglected.

5.1 Simulation of Favres experiments using a dispersive model

The KdV equation was given in (3.22). An equation of the same approximation is reached by interchanging $\eta_x = \frac{\eta_t}{c_0}$. In this way we get the BBM equation.

$$\eta_t + c_0(1 + \frac{3}{2}\frac{\eta}{H_0})\eta_x - \frac{1}{6}H_0^2\eta_{xxt} = 0 \tag{5.1}$$

This equation is known to be preferable from a numerical point of view. By giving initial values with bore strengths identical to those in Favres experiments and having the bore travel a similar length it is possible to recreate the experiments of Favre. Here we have simulated four of Favres runs numerically in order to compare the dispersive model with experimental values. Comparing the simulated values with the experimental values the largest difference is found in the wave length. Favre found the wave lengths to shorten with bore strength, the same does not happen to these simulated bores.

Under the assumption that the simulated flow has obtained a steady flow behind the bore front we can do the same calculation as Sturtevant. Comparing the calculations from the simulated bore with the calculations of the experimental bore gives two interesting observations. Firstly the modulus k^2 is closer to 1 for the simulated data then for the experimental data. This is indicating that the waves in the simulated data are closer to solitary form. Also we find that that the fraction $\frac{r}{r_1} > 1$ in all the simulated runs. This observation casts doubt on Sturtevants result. For the simulated bore we can not draw the conclusion that the fluid is experiencing friction at the bottom, since frictional effects are not part of the model. Our conclusion must be

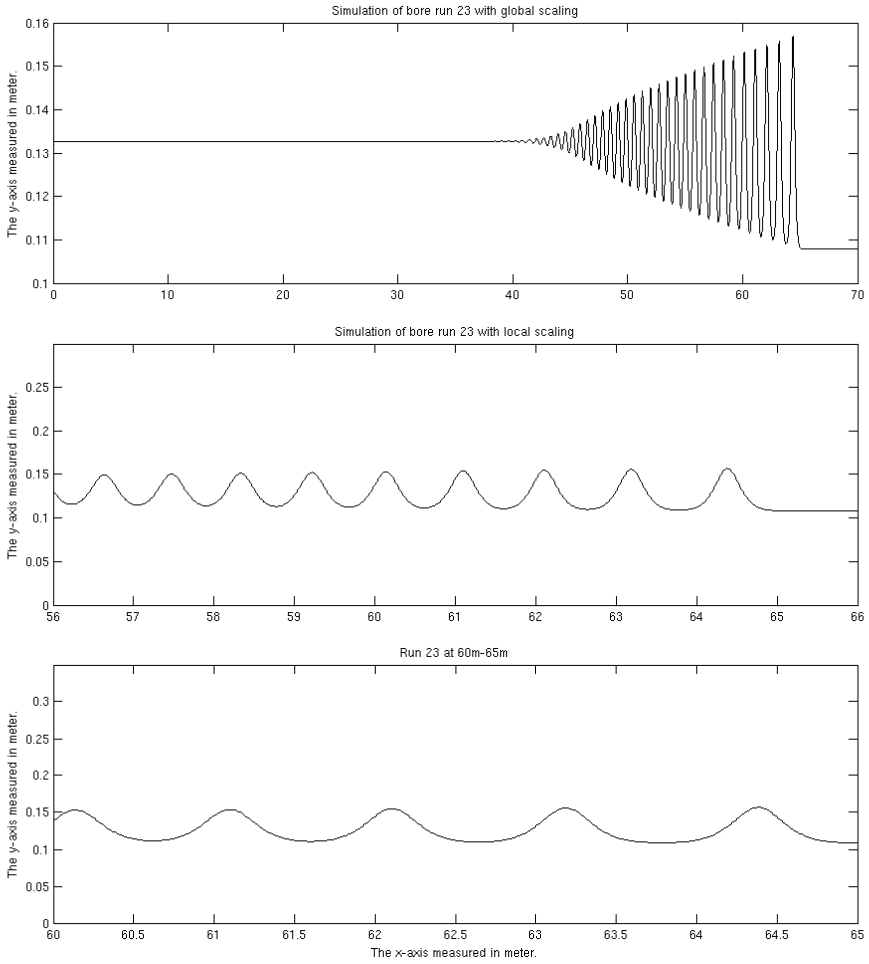

Figure 5.1: These three plots shows the surface of the bore in run 23, having travelled approximately 65 meters down the channel. All the plots are of the same bore at the same time but with different scaling at the axes. The first plot is in a global scale focusing on the surface deviation and it does not show a stable region *a* suggested by Sturtevant in figure 4.1. The global scale shows that the oscillations differ, indicating that the flow is not steady. In the locally scaled plots, the flow appears to be steady, showing how hard it is to make qualitative judgements from plots alone. According to the theory of Benjamin and Lighthill these undulations should drift apart, becoming more and more solitary.

Table 5.1: Measurements of simulated bores: This table presents the numerically measured equivalent of Favres measurements in table 4.1. The values h_1 and h_2 are set identically to the values in Favres experiments and the values w_1, w_2 and Λ are the measurements of wave crest, wave trough and wave length of the first oscillation behind the bore front, as the bore has travelled 65m down the channel.

Run no	h_1	h_2	w_1	w_2	Λ
22	1.073	1.223	1.270	1.013	12.02
23	1.079	1.327	1.455	1.011	11.12
24	1.074	1.376	1.563	1.009	11.17
26	1.075	1.478	1.783	1.005	11.16

Table 5.2: Calculations from measurements of the simulated bores: These are the calculated results from the measurements presented in table 5.1. Most important is column 3 which indicate that also for the simulated bore the fluid picks up energy as it passes through the bore front. This can not be explained by frictional effects and casts doubt on the assumption of steady flow for the bore expressed by the dispersive model.

Run no	k^2	w_3	$\frac{r}{r_1}$	$\frac{r-r_2}{r_1-r_2}$
22	0.8821	0.9788	1.0008	3.05
23	0.9329	0.9791	1.0014	1.98
24	0.9550	0.9829	1.0014	1.55
26	0.9752	0.9852	1.0021	1.09

that, using a dispersive model, the bore flow does not become steady and the apparent energy gain through the bore front is a dynamical effect of the dispersive model.

5.2 Conservation of energy in the dispersive model

Benjamin and Lighthill proves that the surface waves of a steady flow in non-viscous shallow water is given by the relation in (4.9). This proves that the three properties Q, R and S determine the surface waves. In the case of the bore the values of Q, R and S are known up stream of the bore

front. Starting from these values a loss of energy in the region of zero to the classical energy loss, gives a spectre of different surface waves at the front from solitary, cnoidal, sinusoidal to none respectively. Favres experimental results showed that the undulations behind the bore front were steady and Keulegan and Pattersons found the undulations to be cnoidal. From this Benjamin and Lighthill concluded that in order to achieve such undulations the flow was losing energy of about 20% of the classical energy loss through the bore front.

The model used is a non-viscous dispersive system and simulations of Favres experiments show that, using such a model, the simulated bore does not obtain a steady flow in the same region of the channel as the experimental bore. This does not invalidate Benjamin and Lighthills result that Q, R and S determine the the surface waves of a steady flow in a dispersive system, only its application on the experimental bore.

This error in method seems to come from a will to connect the classical energy loss of the turbulent bore to the undular bore. The energy loss in the turbulent bore is an instantaneous energy loss connected to the discontinuity of the bore front. In this way it differs from any energy loss through frictional effects. It might be that the investigations of the undular bores are better served if the concept of the classical energy loss is dismissed all together as a relic of the shallow water system.

To back up this statement we will present two arguments claiming that the need for the classical energy loss disappears as we go from the travelling discontinuity to the dispersive model.

5.2.1 Rayleighs removal of the classical energy loss

Most cites to Rayleighs paper [17] refer to it as the paper introducing the classical energy loss. This is however an inaccuracy as the loss was included only to rectify an earlier publication. The following investigation was the main motivation for the paper. We deduced (2.13)

$$(\frac{u_1^2}{H_0} \cdot \frac{1+\eta_0/2H_0}{(1+\eta_0/H_0)^2} - g)\eta_0 = 0$$

as the condition for the free surface. It could be satisfied only if $\frac{\eta_0}{H_0}$ could be neglected. Here Rayleigh writes: *Although a constant gravity is not adequate to compensate the changes of pressure due to acceleration and retardation in a long wave of finite height, it is evident that complete compensation is attainable if gravity be made a suitable function of height; and it is worth while to enquire what the law of force must be in order that long waves of unlimited*

height may travel with type unchanged. He found that if he let gravity be a function of height $f(z)$ the condition of constant surface pressure became

$$\frac{1}{2}u_1^2\left\{1-\frac{\eta_0^2}{(\eta_0+H_0)^2}\right\}=\int_0^{\eta_0} f dh \tag{5.2}$$

whence

$$f=-\frac{u_1^2}{2}\cdot\frac{d}{dh}\frac{\eta_0^2}{(\eta_0+H_0)^2}=u_1^2\frac{\eta_0^2}{(\eta_0+H_0)^3}. \tag{5.3}$$

The force must vary inversely as the cube of the distance from the bottom. Take note of Rayleighs remark: *It may be remarked that we are concerned only with the values of f at water-levels which actually occur. A change in f below the lowest water level would have no effect upon the motion, and thus no difficulty arises from the law of inverse cube making the force infinite at the bottom of the channel.*

The main reason why this part of Rayleighs paper is uncommented must be that the intensity of gravity is not a function of height. This assumption appears non-physical. However gravity's role in the Euler equation is to determine the pressure in the fluid. Rayleighs approach may be interpreted, not as modifying gravity as such, but as a modification of the pressure. What is interesting about this approach is that it now allows for waves of any heights to travel in shallow water without braking in the same way as with the dispersive models.

Rayleigh further study the energy loss under the same condition. Let gravity be replaced by a force f, which is a function of height. This leads to the following expressions for the pressure.

$$p_1=\textstyle\int_z^{h_1} f dz,\quad p_2=\int_z^{h_2} f dz \tag{5.4}$$

We use these when we rewrite (2.15)

$$\begin{aligned} Q(u_1-u_2)&=\int_0^{h_2} p_2 dz-\int_0^{h_1} p_1 dz\\ &=[p_2 z]_0^{h_2}-[p_1 z]_0^{h_1}-\int_0^{h_2} z\frac{dp_2}{dz}dz-\int_0^{h_1} z\frac{dp_1}{dz}dz\\ &=\int_0^{h_2} z f dz-\int_0^{h_1} z f dz=\int_{h_1}^{h_2} z f dz, \end{aligned} \tag{5.5}$$

where the integrated terms vanish at the limits. In summing up the energy loss both the potential energy and the work done by pressure is changed if

gravity is a function of height, however the difference in kinetic energy is unaffected. Let dE be the energy loss. Rayleigh show that the loss becomes

$$dE = Q\left\{\frac{1}{2}u_1^2 - \frac{1}{2}u_2^2 - \int_{h_1}^{h_2} f dz\right\}. \tag{5.6}$$

This is the classical loss if $f = g$. However if $f = \mu z^{-3}$, with (2.11) and (5.5) giving $\mu = u_1^2 h_1^2 = u_2^2 h_2^2$, the energy loss disappears. This same expression of gravity that gave travelling waves in shallow water also gives no energy loss. In section (3.1) we deduced a dispersive system (3.19) where the term $-\frac{1}{3}(\beta)\tilde{u}_{xxt}$ was this systems improvement on the shallow water system (2.9). In [16] Peregrine writes about this term: *It expresses the effect of the vertical acceleration of water on the pressure. It is absent in Airy's theory*[1] *where the pressure is taken to be hydrostatic.* If it is possible to show that its effects on pressure is approximately[2] the same as the effects of letting gravity vary inversely as the cube of the distance from the bottom of the channel, this would prove that the dispersive models conserve energy.

5.2.2 Numerical study showing the conservation of energy in the dispersive model.

In a recent paper [1] Alfatih and Kalisch published a numerical study of the dispersive system

$$\begin{aligned} h_t + (wh)_x + \tfrac{H_0^3}{6} w_{xxx} &= 0 \\ w_t + gh_x + ww_x + \tfrac{gH_0^2}{6} h_{xxx} &= 0 \end{aligned} \tag{5.7}$$

which can be deduced from (3.15). Here w is the horizontal velocity at the height $\sqrt{\frac{2}{3}H_0}$ and $h(x,t) = \eta(x,t) + H_0$ is the total depth. Also $h_t = \eta_t$ and $h_x = \eta_x$ meaning that depth changes are given by surface changes. The energy between two cross-sections of the channel in this system is

$$E_{disp} = \frac{1}{2}\int_{x_1}^{x_2} \left\{hw^2 + gh^2 + \frac{H_0^3}{3} w w_{xx} + \frac{H_0^3}{3} w_x^2\right\} dx. \tag{5.8}$$

Using this energy integral they could study bore like initial conditions

$$\eta(x,0) = \tfrac{1}{2}a_0[1 - \tanh(kx)], \quad w(x,0) = \tfrac{1}{2}u_0[1 - \tanh(kx)] \tag{5.9}$$

[1] By Airy's theory is meant what we know as the shallow water system.

[2] Approximately in this context meaning to the same degree of accuracy as the dispersive model is derived.

and calculate the energy change in a control volume containing the bore front. They found that the change of energy inside the control volume subtracted the net flux was always zero.

$$\frac{dE_{disp}}{dt} - (F_1 - F_2) = 0. \tag{5.10}$$

This suggests that, in addition to mass and momentum, the dispersive system conserves energy.

Chapter 6

Summary, Conclusion and further work

6.1 Summary

In this thesis we have given an introductory treatment of the bore phenomenon with the main focus on the undular bore. We have restricted the study to a narrow channel of shallow water. Keeping the channel narrow has allowed us to neglect any flow transversely to the channel, thereby turning the water flow into a two dimensional entity with a flow in the vertical direction and a horizontal flow in the direction of the channel. In regarding water as an ideal fluid we have made two major simplifications. Foremost of these is the treatment of water as non-viscous removing all frictional effects. But also the assumption of water as homogeneous and incompressible is useful as a constant density absolves the need for the internal thermodynamic considerations of water. This procedure of simplifications was justified by our objective of giving a general and simple account of the bore phenomenon.

At the outset we assumed that the waves were long compared to the depth of the channel. This led us to assume that we could neglect vertical flow. Without vertical flow the pressure would be hydrostatic as given in (2.7) and the shallow water equations (2.9) followed. We studied this system as a system of non-linear advection equations and found that it could not attain travelling wave solutions. All surface waves of this system would form a discontinuity and break. We established a weak solution (2.32) for the system, modelling the bore as a travelling discontinuity with shock speed U. In section (2.5) we calculated (2.45) which showed that this bore, conserving mass and momentum, had an energy loss through the front. This calculation provided the connection between the hydraulic jump and the bore and might

have led one to believe that all bores experience some form of turbulent dissipation.

Favre's experiments revealed that also non-turbulent bores exist. These bores carry a train of undulations behind the bore front and are called undular bores. Such undulation being incompatible with the shallow water system motivated the need for a dispersive system. A more detailed description of the fluid velocity using the velocity potential ϕ lead to this system. The dispersive system was deduced for moderately small wave amplitudes and moderately long wave lengths, that is both $\alpha = \frac{a}{H_0}$ and $\beta = \frac{H_0^2}{\lambda^2}$ were small but not insignificant. Studying the KdV equation (3.22), a specialized form of the dispersive system, where the flow moves in one direction, we found that several travelling wave solutions were possible.

Benjamin and Lighthill derived the equation for travelling wave solutions of a dispersive system in a way that illuminated the roll of mass flux, momentum flux and energy. They found, from the flow conditions up stream of the bore front, that an undular bore attaining a steady flow without the loss of energy or momentum would display a solitary wave rather then a train of undulations. Since experimental data suggested that the undulations were cnoidal waves they postulated that the undular bore suffered an energy loss.

Using the BBM equation to simulate bore-like initial values showed that the dispersive system display the bore as a travelling front carrying a train of undulations much like the undular bore. However the experimentally found steady flow of the undular bore was not reflected in the simulated undular bore. Assuming steady flow for the simulated bore and repeating the calculations done by Sturtevant on the experimental bore showed that the bores of the dispersive systems do not obtain steady flow in the same region as the experimental bores of Favre.

The classical energy loss (2.17) derived by Rayleigh suggests that the bore carry an amount of energy which it in some cases liberate through turbulence at the bore front. This energy loss was repeatedly referred to by Benjamin and Lighthill and they proposed that different degrees of energy loss within the domain of the classical energy loss would be reflected in different types of surface waves behind the bore front. The final part of the thesis present two arguments which claim that the dispersive system posses a dynamical effect capable of conserving this energy within the fluid. This leads us to think that any energy loss sustained by an undular bore is independent of the classical energy loss predicted for the shallow water system.

6.2 Conclusion

Benjamin and Lighthill concluded that the physical values Q, R and S determined the surface waves of a steady flow in a dispersive system. They applied this to the bore and based on Favres experimental measurements of its surface waves deduced that the bore needed to dissipate some energy. Specificity they write: *For a bore with no frictional effects at all, any wave-train produced (whatever the intervening motion in the neighbourhood of the bore) must have Q, R and S equal to the values which they take upstream. But the only wave with these values for Q, R and S is the solitary wave.... The solitary wave must therefore be the unique wave which can appear out of a uniform motion without frictional action.*

Any simulation of the bore using a dispersive system will model a bore experiencing no frictional effect. As we simulate the bore we find that a train of waves appear behind the bore front. The explanation for this is that Benjamin and Lighthill does not address the transitional phase where the flow goes from the unsteady initial discharge wave to the steady solitary wave. Taking note of this we understand that the solitary wave profile predicted by Benjamin and Lighthill is the profile reached as time goes to infinity. This shows, as we have pointed out, that the stabilizing effect found experimental is not reflected in the dispersive model.

In Favres experiments the bore is said to obtain a steady flow and the measurements are taken only 65 meters from where the bore is generated. This should be the main argument for why the dispersive model is not satisfactory as a model for the undular bore. Shifting the focus from the energy dissipation of the flow to stability conditions of it should be very useful when searching for the new model. When including frictional effects, a study of the steadying effect would determine the success of the model. Measuring if a flow is stable should be simple since Q needs to be constant at any vertical cross-section of the flow. Once bore models that quickly obtain steady flow are provided a study along the line of Benjamin and Lighthills would determine which of the models are best from a surface wave perspective.

The classical energy loss found for the turbulent bore has been subject of discussion. This energy amount is connected to the fluids transition between the two uniform flow depths of the bore. In the simplest model we assumed that energy instantly disappeared, in form of turbulence, as the fluid passed through the front. We have argued that the dispersive system, allowing flow in the vertical direction, has given the flow dynamical effects, in form of wave motion, able to conserve this energy otherwise turbulently dispersed. In searching of a new model the classical energy loss will represent the maximum amount of energy dissipation allowed without simultaneously altering the

horizontal momentum of the flow, however the model should not focus on satisfying any energy loss condition as such.

6.3 Further work and the search for a new model

Through out this treatment there has risen several issues that requires further attention, and tasks of analytical, numerical and experimental nature lies ahead.

The main analytical task is to include frictional effects in the dispersive model. With this new model for the bore there will be a need to repeat Benjamin and Lighthills work where frictional effects are taken into account. In addition we suggested a connection between Rayleighs treatment of gravity as a function of height in the shallow water system and the dispersive modification of this system. Proving such a relation would be a nice result from which the conservation of energy in the dispersive system could be confirmed.

Numerically we should verify the results of Benjamin and Lighthill by showing that bore like initial values eventually establish solitary waves behind the bore front. Also in developing the new model, numerics will be essential in checking that this model obtains a stable flow.

Experimentally we should study the steadiness of the bore. Modern technology, using super cameras, gives an improved ability to measure the bore as it travels down its channel. This should allow us confirm whether the bore obtains a steady flow, measure how quickly it does so, and determine whether the waves behind the bore front are of a cnoidal character.

Many of the suggestions raised here have already been undertaken. On adding frictional effects to the dispersive model a good starting point would be to expand on the analytical and numerical work done by Chester [6], Byatt-Smith [5] and Johnson [10]. In addition newer experimental results are being published where the use of modern measuring techniques are improving the data. Whether these focus on steady flow should be investigated. But even if good experiments have been done, anyone seeking deeper understanding of the bore phenomenon needs to do physical testing themselves.

Appendix A

This appendix gives a short description of the finite difference schemes behind the numerical algorithm, applying the BBM equation on bore like initial values in chapter 5.

A.1 The numerical method

The aim is to make a numerical algorithm that can be used in simulating a one-dimensional propagation of a bore along a channel. A bore will be given as an elevation a_0 traveling to the right into undisturbed water of depth H_0. The commonly used initial value for a bore is

$$\eta_0 = \left(\frac{a_0}{2}\right)(1 - \tanh(kx))$$

where k is a parameter for the initial steepness of the elevated water. The algorithm will treat the bores on a finite domain for a finite time. The domain will be sufficiently large for us to assume that the flow up and down stream of the propagating bore is uniform. Since the fluid flow is uniform at the boundary its surface will take constant values there. We will describe this by giving Dirichlet boundary conditions for η at these boundary points. For solitary waves the boundary conditions are homogeneous with $\eta = 0$ at the boundary. For propagating bores the boundary conditions are non-homogeneous. The left boundary is the the deviation from the surface of undisturbed depth i.e. a_0 and the right boundary is the surface of undisturbed depth i.e. 0. Note that constant values of η at the boundary imply that $\eta_t = 0$ at the boundary.

The foundation of the numerical algorithm solves the dimensionless BBM equation:

$$\eta_t + \left(\eta + \eta^2\right)_x - \eta_{xxt} = 0 \tag{A.1}$$

The equation is better approached if we order the t derivatives on the left hand side.

$$\eta_t - \eta_{xxt} = -\left(\eta + \eta^2\right)_x \tag{A.2}$$

It is a natural choice to deal with the x derivatives by a finite difference scheme. We discretise the spacial dimension into a set of equidistant grid points where Δ_x represents the distance between the grid points. In this case $\frac{\partial}{\partial x} = \frac{1}{\Delta_x}\,\Upsilon_0\,\triangle_0 + O(\Delta_x^2)$ and $\frac{\partial^2}{\partial x^2} = \frac{1}{\Delta_x^2}\,\triangle_0^2 + O(\Delta_x^2)$ where $\triangle_0$ is the central difference operator and Υ_0 is the averaging operator. This is the notation used in [9]. Our numerical expression for the BBM equation then becomes

$$\left(I - \frac{\triangle_0^2}{\Delta_x^2}\right)\eta_t = -\frac{\Upsilon_0\triangle_0}{\Delta_x}\left(\eta + \eta^2\right) \tag{A.3}$$

With an initial value for η, the right hand side of the equation (A.3) is possible to calculate. Thus we can view (A.3) as an equation of the form

$$A\eta_t = b$$

where the η_t is the unknown with the solution:

$$\eta_t = -\left(I - \frac{\triangle_0^2}{\Delta_x^2}\right)^{-1}\frac{\Upsilon_0\triangle_0}{\Delta_x}\left(\eta + \eta^2\right) \tag{A.4}$$

When we have solved for η_t, it is a straightforward process to apply Heuns method, a second order Runge-Kutta method, to approximate the time evolution of the equation.

A.1.1 Implementing the algorithm.

The overall idea for the solver was explained above. Implementing the solver turns our attention to practical details. On inspection the algorithm can be divided into three parts, which can be treated individually. One is the calculation of the $-\frac{\Upsilon_0\triangle_0}{\Delta_x}\left(\eta + \eta^2\right)$ term. Two is the solving the linear equation $A\eta_t = b$. Three is the application of Heuns method.

The $-\frac{\Upsilon_0\triangle_0}{\Delta_x}\left(\eta + \eta^2\right)$ term.

Since we are given an initial value it is possible to calculate $-\frac{\Upsilon_0\triangle_0}{\Delta_x}\left(\eta + \eta^2\right)$. Let η_k denote the value of η at the k-th grid point. Then by our approximation $\frac{\partial \eta_k}{\partial x} = \frac{\eta_{k+1} - \eta_{k-1}}{2\Delta_x}$ and similarly for η^2. With a discretization of the x-dimension in n grid points we get a vector u of n components for η. This approximation can be expressed by vector manipulation. Here is a simple Matlab code:

```
temp=[bl, u, br];
temp=temp+temp.^2;
f=-(temp(3:end)-temp(1:end-2))/(2*dx);
```

Here temp is a temporary vector, bl and br are left and right boundary value, dx is Δ_x and

$$f = -\frac{\Upsilon_0 \triangle_0}{\Delta_x}\left(\eta + \eta^2\right)$$

This code reveals that the vector u, approximating η, does not itself contain the boundary values. These are added temporarily when the approximation of the x derivative is calculated. In this way the boundary values are kept constant.

Using the linear equation $A\eta_t = b$ to solve for η_t.

Having calculated the $-\frac{\Upsilon_0 \triangle_0}{\Delta_x}(\eta + \eta^2)$ term we have determined the right hand side of the equation. Now we concentrate on the matrix $A = \left(I - \frac{\triangle_0^2}{\Delta_x^2}\right)$. Finite difference gives the following approximation of the double derivative

$$\frac{\partial^2 z_k}{\partial x^2} = \frac{z_{k+1} - 2z_k + z_{k-1}}{\Delta_x^2} + O(\Delta_x^2)$$

where z is some arbitrary vector. It follows that A is tridiagonal where the diagonal terms are $I + \frac{2}{\Delta_x^2}$ and the -1 and $+1$ diagonals are both $\frac{-1}{\Delta_x^2}$. This means that A can be expressed as a combination of three vectors. The solutions of such tridiagonal systems are fairly simple and a solving routine, called trisolv, was made based on the recipe given in [12] page 180. The boundary gives no contribution in this calculation as $\eta_t = 0$ at the boundary.

Time evolution with Heuns method.

Having found how the surface deviation η is momently changing with time, i.e. the η_t terms, we can calculate a time step of η. As our approximations so far are of second order it is reasonable to use a second order routine for this prediction as well. To do this we employ the Heun method. This is a modification of Eulers method. Eulers method states our simplest intuition: Let $s = 1, 2 \cdots, n$ be the number of time-steps taken. Then a future value of η, denoted as η_{s+1}, is given by a present value of η, denoted η_s, plus some change with time given by $(\eta_s)_t \Delta_t$ where Δ_t is our time step. This gives

$$\eta_{s+1} = \eta_s + (\eta_s)_t \Delta_t + O(\Delta_t^2) = \widehat{\eta}_{s+1} + O(\Delta_t^2)$$

If $(\eta_s)_t$ does not change during the time step then this is exactly true.

Heuns method improves on Eulers method in that it gives an approximation to how $(\eta_s)_t$ does change with time. This is done by first taking a step with Eulers method giving

$$\eta_{s+1} = \widehat{\eta}_{s+1} + O(\Delta_t^2).$$

Using this expression in (A.4) we get

$$(\eta_{s+1})_t = (\widehat{\eta}_{s+1})_t + O(\Delta_t^2)$$

Assuming that this process does not effect the order with respect to Δ_t. By derivating Eulers method with respect to t we get:

$$(\eta_{s+1})_t = (\eta_s)_t + (\eta_s)_{tt}\Delta_t + O(\Delta_t^2) = (\widehat{\eta}_{s+1})_t + O(\Delta_t^2)$$

giving the following:

$$(\eta_s)_{tt} = \frac{(\widehat{\eta}_{s+1})_t - (\eta_s)_t}{\Delta_t} + O(\Delta_t)$$

estimate for $(\eta_s)_t$s change with time. This leads to an equation for Heuns method.

$$\eta_{s+1} = \eta_s + \frac{1}{2}\left[(\eta_s)_t + (\widehat{\eta}_{s+1})_t\right]\Delta_t + O(\Delta_t^3) \tag{A.5}$$

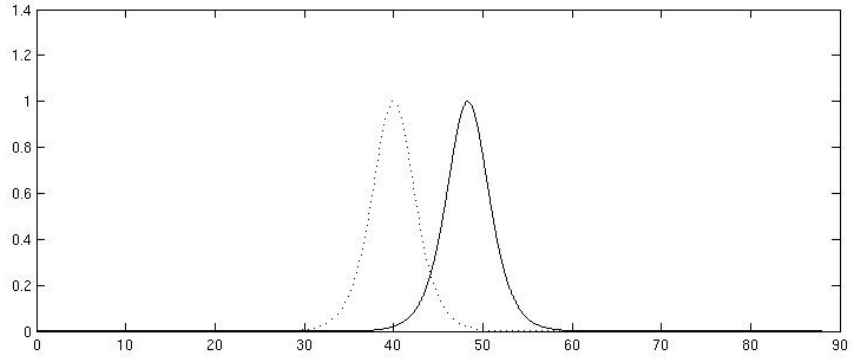

Figure A.1: Here is the solitary wave, used in the convergence testing, propagating to the right. The dotted figure is the initial wave.

A.2 Testing convergence.

As mentioned in the development of the KdV equation,

$$\eta_t + \left(\eta + \eta^2\right)_x - \eta_{xxt} = 0$$

has exact solitary-wave solutions. The solutions are of the form

$$\eta(x,t) = a\text{sech}^2\left\{\left(\frac{a}{4a+6}\right)^{\frac{1}{2}}\left[x - \left(1+\frac{2}{3}a\right)t\right]\right\} \tag{A.6}$$

where $a > 0$ is a parameter specifying the amplitude (and the speed) of the wave, see [4]. Using these exact solutions we can test the convergence of the algorithm.

The test used a solitary wave, seen in figure 1, with amplitude $a = 1$, centred at $x = 40$ at initial time $t_0 = 0$ as initial value. The homogeneous boundary conditions $\eta = 0$ was used at the left and right boundary points. The wave traveled to $t = 5$. The interval of x, $x \in [0, 28\pi]$, was chosen such that the wave never had a value exceeding 10^{-10} close to the interval endpoints. At the first test the discretization of the x-axis was kept constant at $\Delta_x = 0.001$ while the time steps were halved from $\Delta_t = 0.1$ to $\Delta_t = 0.003125$. In the second test the roles of Δ_t and Δ_x was reversed. The result are stored in the two following tables.

Table A.1: Convergence test for Δ_t with fixed Δ_x

Δ_x	Δ_t	L_∞ **-error**	**ratio**
0.001	0.100000	367.92e-05	
0.001	0.050000	92.27e-05	3.99
0.001	0.025000	23.10e-05	3.99
0.001	0.012500	5.77e-05	4.00
0.001	0.006250	1.44e-05	4.02
0.001	0.003125	0.35e-05	4.10

These results suggest that the algorithm has second order convergence with respect to Δ_x and Δ_t.

Table A.2: Convergence test for Δ_x with fixed Δ_t

Δ_x	Δ_t	L_∞ **-error**	**ratio**
0.100000	0.001	115.12e-05	
0.050000	0.001	28.78e-05	3.99
0.025000	0.001	7.17e-05	4.01
0.012500	0.001	1.76e-05	4.06
0.006250	0.001	0.41e-05	4.26
0.003125	0.001	0.08e-05	5.47

Bibliography

[1] A. Ali and H. Kalisch. Energy balance for undular bores. *Comptes Rendus Mécanique*, 2010.

[2] H. Bazin. Recherches experimentales sur la propagation des ondes. *Experimental Research on Wave Propagation.') Mémoires présentés par divers savants à l'Académie des Sciences, Paris, France, Vol. 19, pp. 495-644 (in French)*, 1865.

[3] TB Benjamin and MJ Lighthill. On cnoidal waves and bores. *Proceedings of the Royal Society of London. Series A, Mathematical and Physical Sciences*, 224(1159):448–460, 1954.

[4] J.L. Bona, WG Pritchard, and L.R. Scott. Solitary-wave interaction. *Physics of Fluids*, 23:438, 1980.

[5] JGB Byatt-Smith. The effect of laminar viscosity on the solution of the undular bore. *Journal of Fluid Mechanics*, 48(01):33–40, 2006.

[6] W. Chester. A model of the undular bore on a viscous fluid. *Journal of Fluid Mechanics*, 24(02):367–377, 2006.

[7] P. G. Drazin and R. S. Johnson. *Solitons: an introduction*. Cambridge Texts in Applied Mathematics. Cambridge University Press, Cambridge, 1989.

[8] H. Favre. *Etude théorique et expérimentale des ondes de translation dans les canaux découverts*. Dunod, 1935.

[9] A. Iserles. *A First Coures in the Numerical Analysis of Differential Equations*. Cambridge Texts in Applied Mathematics. Cambridge, 2 edition, 2009.

[10] RS Johnson. Shallow water waves on a viscous fluid-the undular bore. *Physics of Fluids*, 15:1693, 1972.

[11] Garbis H. Keulegan and George W. Patterson. Mathematical theory of irrotational translation waves. *J. Research Nat. Bur. Standards*, 24:47–101, 1940.

[12] D. Kincaid and W. Cheney. *Numerical Analysis: Mathematics of Scientific Computing*. The Brooks/Cole Series in Advanced Mathematics. Brooks/Cole, 3 edition, 2002.

[13] P. K. Kundu and I. M. Cohen. *Fluid Mechanics*. Academic press, 4 edition, 2008.

[14] R. Lemoine. Sur les ondes positives de translation dans les canaux et sur le ressaut ondulé de faible amplitude. *Jl La Houille Blanche*, pages 183–185, 1948.

[15] Randall J. LeVeque. *Numerical methods for conservation laws*. Lectures in Mathematics ETH Zürich. Birkhäuser Verlag, Basel, second edition, 1992.

[16] DH Peregrine. Calculations of the development of an undular bore. *Journal of Fluid Mechanics*, 25(02):321–330, 2006.

[17] L. Rayleigh. On the theory of long waves and bores. *Proceedings of the Royal Society of London. Series A, Containing Papers of a Mathematical and Physical Character*, 90(619):324–328, 1914.

[18] JA Sandover and OC Zienkiewicz. Experiments on surge waves. *Water Power*, 9:418–424, 1957.

[19] B. Sturtevant. Implications of experiments on the weak undular bore. *Physics of Fluids*, 8:1052, 1965.

[20] G. B. Whitham. *Linear and nonlinear waves*. Wiley-Interscience [John Wiley & Sons], New York, 1974. Pure and Applied Mathematics.